Regional Dynamic Traffic Assignment with bounded rational drivers as a tool for assessing the emissions in large metropolitan areas

Sergio Batista, Ludovic Leclercq

Regional Dynamic Traffic Assignment with bounded rational drivers as a tool for assessing the emissions in large metropolitan areas

S. F. A. Batista[a,*], Ludovic Leclercq[b,**]

[a]*Division of Engineering, New York University Abu Dhabi, United Arab Emirates*
[b]*Univ. Gustave Eiffel, Univ. Lyon, ENTPE, LICIT, F-69518, Lyon, France*

Abstract

Data-driven surveys show that drivers do not always choose the shortest-path for their travels. The ideas of bounded rationality have been used to model this behavior, and relax the main assumption of travel time minimization of the *User Equilibrium* principle. In this paper, we propose an extension of an existing dynamic traffic assignment framework, for aggregated traffic models based on the Macroscopic Fundamental Diagram and regional networks, that extends the principle of the *User Equilibrium* to account for bounded rational drivers. We focus on drivers with indifferent preferences, and with preferences for more reliable travel times. The network equilibrium is calculated through Monte Carlo simulations and the classical Method of Successive Averages. We first investigate how the drivers' preferences for reliable travel times influences the traffic dynamics in the regional network. We then discuss a potential application example of the proposed methodological framework for estimating the emissions of Carbon Dioxide CO_2 and Monoxide NO_x at the network level. The results shed light on the importance of properly accounting for more realistic drivers' behavior for estimating emissions. The main contributions of this study lie on the edge between the disciplines of traffic flow theory and network modeling, with a great potential of application for practitioners to assess traffic emissions on large metropolitan areas.

Keywords: regional dynamic traffic assignment, Macroscopic Fundamental Diagram, bounded rational drivers, value of reliability, emissions

Highlights

- We propose an extension of a Regional Dynamic Traffic Assignment model that accounts for bounded rational drivers.
- We consider drivers with indifferent preferences and preferences for reliable travel times.
- Monte Carlo simulations are used to account for uncertainty on the trip lengths and traffic dynamics in the regions.
- We show that the Value of Reliability has a significant influence on the traffic dynamics during the congested periods.
- We show that the total concentrations of CO_2 and NO_x increase as the Value of Reliability also does.

1. Introduction

The aggregated traffic models attracted more interest from the traffic flow theory community after the works of Daganzo (2007) and Geroliminis and Daganzo (2008). For this kind of traffic models, the city network depicted in

*Corresponding author. Tel. : +971 26 28 76 98, sergio.batista@nyu.edu
**Corresponding author. Tel. : +33 (0) 4 72 04 77 16, ludovic.leclercq@univ-eiffel.fr

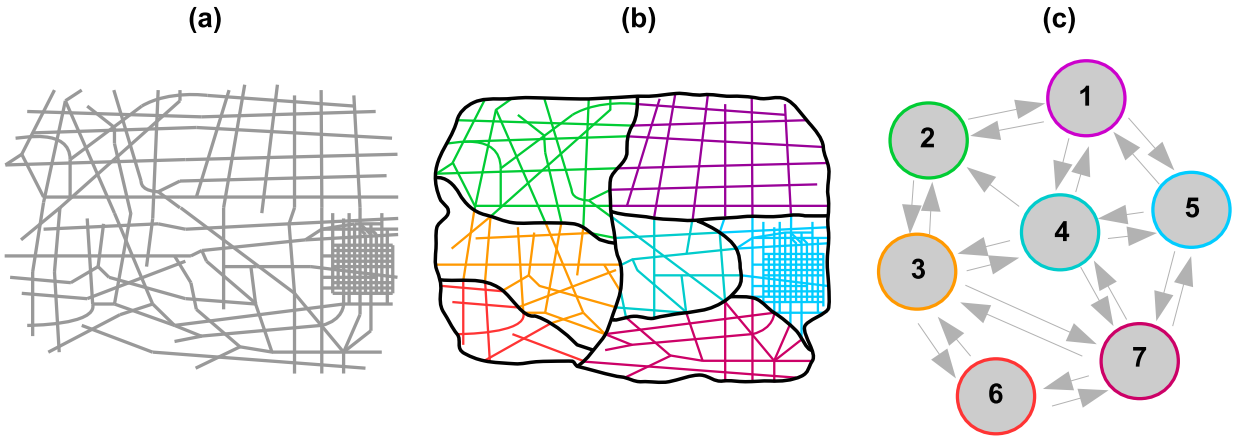

Figure 1: (a) City network. (b) Partition of the city network. (c) Regional network.

Figure 1 (a) is partitioned into regions (Figure 1 (b)), where the traffic conditions are approximately homogeneous. The partitioning can be done using any of the approaches discussed in the literature (e.g. Saeedmanesh and Geroliminis, 2016; Lopez et al., 2017; Saeedmanesh and Geroliminis, 2017; Casadei et al., 2018; Ambühl et al., 2019). Let X be the set of regions. In each region, the traffic conditions are governed by a Macroscopic Fundamental Diagram (MFD). The MFD is a relationship between the average circulating flow of vehicles q_r ([veh/s]) and the accumulation n_r ([veh]) in a given region r. The evolution of the traffic dynamics, n_r, depends on the balance between the inflow $Q_{in,r}(t)$ and outflow $Q_{out,r}(t)$, for each region $r \in X$:

$$\frac{dn_r(t)}{dt} = Q_{in,r}(t) - Q_{out,r}(t), t > 0 \tag{1}$$

In the literature, one can distinguish between two MFD-based models. The accumulation-based model (Daganzo, 2007; Geroliminis and Daganzo, 2008) assumes that the vehicles outflow of a given region r is proportional to an average travel distance $\overline{L}_r$ common to all vehicles traveling in that region, i.e. $Q_{out,r}(t) = \frac{P_r(n_r(t))}{\overline{L}_r}$ where $P_r(n_r(t))$ is the production-MFD. In the case of the trip-based model (Arnott, 2013; Fosgerau, 2015; Lamotte and Geroliminis, 2016; Mariotte et al., 2017; Leclercq et al., 2017; Mariotte and Leclercq, 2019; Vickrey, 2020), the inflow $Q_{in,r}(t)$ and outflow $Q_{out,r}(t)$ are determined by noting that the travel distance L of a vehicle entering a given region r, at time $t - T(t)$ satisfies: $L = \int_{t-T(t)}^{t} \frac{P_r(n_r(s))}{n_r(s)} ds$. We refer the reader to Mariotte et al. (2017) for more details about theoretical background of these two MFD models, as well as their implementation details.

The partition of the city network, depicted in Figure 1 (b), allows to define the regional network (Figure 1 (c)), where routing options are defined. Scaling-up a city into a simpler regional network brings several challenges for dynamic traffic assignment and network loading (Yildirimoglu and Geroliminis, 2014; Batista and Leclercq, 2019a,b). The main reason is related with the definition of paths in the regional network. Figure 2 (a) depicts an example of three trips in the city network. We observe that these three trips cross a different sequences of regions, following the definition of the city network partitioning. This ordered sequence of crossed regions from the Origin to the Destination region is called regional path. Figure 2 (b) shows the two regional paths associated to the three trips. One can also observe that both the green and blue trips have different travel distances inside each region they cross. This defines trip length distributions for each regional path inside each region, contrarily to the links in the city network that have a fixed physical length. Another important aspect is the correlation between regional paths. The correlation dictates the sharing of information between paths and how the path choices of drivers affect each other. Figure 2 (c) zooms the grey region, where the blue and green regional paths are correlated due to the MFD assumption of homogeneous traffic conditions. Inside the grey region, all vehicles travel at the same average speed given by the MFD, independent of their regional path. One vehicle that enters the grey region and travels on the blue regional path will reduce the mean speed of all vehicles traveling on this region due to the MFD assumption of homogeneous speed.

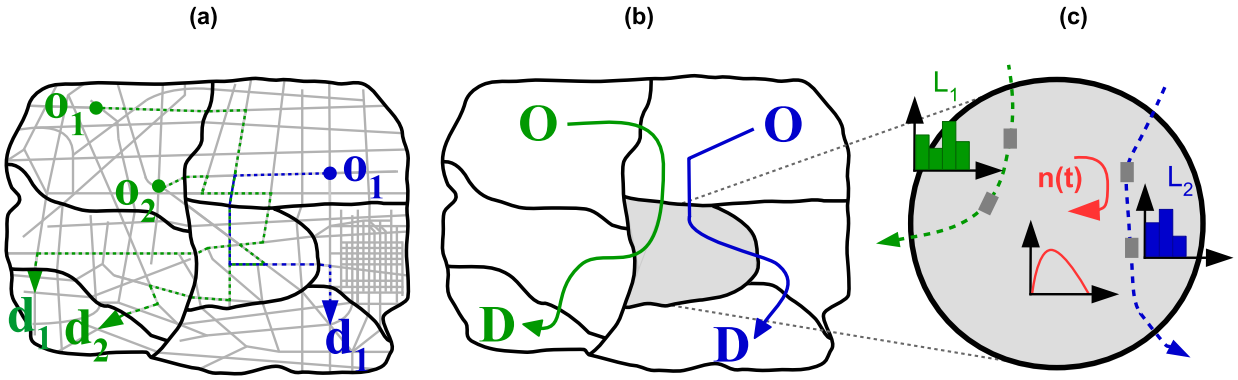

Figure 2: (a) Trips in the city network. (b) Regional paths. (c) Zoom in the grey region.

Up to now, the question of dynamic traffic assignment on regional networks has received little attention in the literature. Yildirimoglu and Geroliminis (2014) are certainly the first that tried to address this question. Their framework is based on the Multinomial Logit model, and therefore does not capture the correlation between regional paths. The trip lengths are also implicitly calculated. Batista and Leclercq (2019b) discuss a regional dynamic traffic assignment framework for MFD traffic models based on the simple User Equilibrium description, but incorporates explicitly calculated trip length distributions as well as the evolution of the regional mean speeds. The authors show that the variability of trips lengths cannot be neglected in the calculation of the regional network equilibrium. The correlation between regional paths can be accounted for through the variability of the regional mean speeds in the dynamic network loading.

Data surveys (e.g. Zhu and Levinson, 2015) show that drivers do not always choose path with the minimal travel times. In this paper, we propose to extend the principle of the *User Equilibrium* to account for bounded rational drivers when calculating the regional network equilibrium. We focus on the regional dynamic traffic assignment framework designed by Batista and Leclercq (2019b), and extend it to consider bounded rational drivers with indifferent preferences (Mahmassani and Chang, 1987; Di and Liu, 2016; Batista et al., 2018) and bounded rational drivers that have preferences for more reliable travel times. We first investigate how the drivers' preferences for travel times reliability influences the traffic dynamics in the regions. We then discuss a potential application example of this R-DTA framework for estimating the emissions of Carbon Dioxide CO_2 and Monoxide NO_x at the regional level. In this matter, we investigate how the different preferences of bounded rational drivers affect the emissions of CO_2 and NO_x. The multidisciplinarity of this paper lies on the edge between two distinct disciplines on traffic and network modeling, i.e. on one side traffic flow theory and on the other econometric/random utility and bounded rationality theories. This paper also shows the great potential of the proposed methodology for assessing traffic emissions in large urban areas.

The remainder of the paper is organized as follows. In Sect. 2, we do a literature review of traffic assignment models in city networks. In Sect. 3, we describe the methodological framework and introduce the proposed extensions to the R-DTA. In Sect. 4, we discuss the influence of the drivers' indifferent preferences and preferences for more reliable travel times on the traffic dynamics in the regions and on the emissions of CO_2 and NO_x at the regional level. In Sect. 5, we outline the conclusions of this paper. In Sect. 6, we provide a general and critical evaluation of the proposed methodological framework, stressing its main advantages and limitations with respect to other approaches in the literature.

2. Dynamic traffic assignment on city networks: a literature review

The initial ideas of traffic assignment date back to the work of Knight (1924). The goal of traffic assignment models is to reproduce the travel patterns in a city network. These models require:

- the definition of the trip choice set Ω^{od}, for each origin-destination (od) pair of the set Ξ of all od pairs in the city network.

- the specification of the utility function U_k^{od} for trip k that connects the od pair.

The first step of traffic assignment models consists in identifying the trip set $\Omega^{od}, \forall (o,d) \in \Xi$. It is composed by trips in the city network that drivers consider for their travels. Note that, trips in the city network are represented by a sequence of links that have a fixed physical length. Several authors propose different models and approaches to determine Ω^{od}, such as the constrained k-shortest paths (van der Zijpp and Catalano, 2005), the link penalty (de la Barra et al., 1993), the link elimination (Azevedo et al., 1993), the labeling approach (Ben-Akiva et al., 1984), the branch-and-bound algorithm (Prato and Bekhor, 2006), the simulation approach (Nielsen, 2000; Nielsen et al., 2002), the sampling of trips (Frejinger et al., 2009; Flötteröd and Bierlaire, 2013) or a dynamic setting of a link-choice based model (Dial, 1971; Fosgerau, 2013).

The next step is related with the setting of the utility function $U_k^{od}, \forall k \in \Omega^{od} \wedge \forall (o,d) \in \Xi$. In general, drivers evaluate their trips choices by balancing the trip monetary cost TC_k^{od} and the perceived travel time TT_k^{od}:

$$U_k^{od} = TC_k^{od} + \beta^{od} TT_k^{od}, \forall k \in \Omega^{od} \wedge \forall (o,d) \in \Xi \tag{2}$$

where β^{od} is the Value of Time (VOT) (e.g. Zhang et al., 2013), that is the marginal cost between the trip monetary cost and its travel time. The monetary costs can be associated with tolls or public transport tickets, to name a few examples.

The first ideas of traffic assignment and network equilibrium were introduced by the two principles of Wardrop (1952). The principle of the User Equilibrium or Deterministic User Equilibrium (DUE) assumes that drivers are selfish and foresee to minimize their own travel times, i.e. drivers have a perfect rationality. In this case, they perceive the exact travel times. But, traffic conditions change over time, originating congestion patterns in the city network that are difficult to predict. This induces uncertainty in the trips travel times. We then rewrite the perceived utility of trip k, U_k^{od}, to include the uncertainty term ϵ_k^{od} as:

$$U_k^{od} = \overline{TT}_k^{od} + \epsilon_k^{od}, \forall k \in \Omega^{od} \wedge \forall (o,d) \in \Xi \tag{3}$$

where $\overline{TT}_k^{od}$ is the average travel time for trip k; and ϵ_k^{od} is the uncertainty term or, as often referred to in the literature, the error term. In this case, the city network equilibrium corresponds to the Stochastic User Equilibrium (SUE) (Daganzo and Sheffi, 1977; Daganzo, 1982). Random Utility theory (McFadden, 1978) is usually used to incorporate ϵ_k^{od} in the modeling of drivers trip choices. One can distinguish between two main groups of Random Utility models applied to traffic assignment: the group of the Logit models (Chen et al., 2012; Cascetta et al., 1996; Ben-Akiva and Bierlaire, 1999; Bovy et al., 2008; Prashker and Bekhor, 2000; Bekhor and Prashker, 2001; Prashker and Bekhor, 1998); and the group of the Probit model (Daganzo and Sheffi, 1977). The latter model is only used in few applications in the literature. The main reason is because this model requires the integration of a multi-normal variate distribution over the number of trips connecting the od pair, requiring a large computational cost. One solution is to solve these integrals through Monte Carlo simulations (Sheffi, 1985). For this, one has to discretize the trip travel times into several realizations or draws and locally solve deterministic assignment problems. The final choices correspond to the average of all local choices.

The previous definitions of the network equilibria have been extended in two directions to incorporate different kinds of drivers' behavior as well as heterogeneous drivers. We first focus on the relevant literature that discusses extensions of traffic assignment models for different kinds of drivers' behavior. The utility minimizers assumption of the *User Equilibrium* is then relaxed to account for bounded rational drivers. The concept of bounded rationality was introduced to the economic field by Simon (1957, 1966, 1990, 1991). These ideas were later adapted to the context of traffic assignment by Mahmassani and Chang (1987), Di et al. (2013, 2014) and Di and Liu (2016). Drivers choose any trip(s) of which the perceived utility U_k^{od} is/are inferior to a pre-defined threshold called the Aspiration Level AL^{od}, i.e. $U_k^{od} \leq AL^{od}, \forall (o,d) \in \Xi$. This behavior is coined as *satisficing*, which results from the concatenation of the words suffice and satisfy. By other words, the driver(s) is/are satisfied if the travel time of their chosen trip(s) is inferior to the AL^{od}. The Aspiration Level AL^{od} is calculated through the definition of the indifference band Δ^{od} (Mahmassani and Chang, 1987):

$$AL^{od} = \min(\vec{V})(1 + \Delta^{od}), \forall (o,d) \in \Xi \tag{4}$$

where $\vec{V}$ is the vector containing all average travel times of all regional paths listed in Ω^{od}. The question now is how drivers are assigned to the *satisficing* trips. Batista et al. (2018) assigned drivers to *satisficing* trips based on indifferent and strict preferences. In this paper, we target bounded rational drivers with indifference preferences (Batista et al., 2018). In this case, the demand of each od pair is equally split over all *satisficing* trips. Other studies focused on regret-averse drivers (Chorus, 2012a,b, 2014; Li and Huang, 2016), where they aim to minimize their own regret in relation to the unselected trips. Kazagli et al. (2016) presented an innovative methodological framework where traffic is assigned according to mental representations (MRIs) of drivers.

We now focus on the relevant literature that discusses the extensions of traffic assignment models to heterogeneous users. The drivers' heterogeneity is included in the definition of the utility function $U_k^{od}, \forall k \in \Omega^{od} \wedge \forall (o,d) \in \Xi$ through the Value of Time (VOT) (e.g. Dafermos, 1972; Smith, 1979; Dafermos, 1980, 1982) and/or the Value of Reliability (VOR) (e.g. Jackson and Jucker, 1982; Small, 1982). In this paper, we focus on the latter. The literature there are several models that incorporate the VOR, such as the mean-variance model (Jackson and Jucker, 1982), the scheduling-delay (Small, 1982), the late-arrival penalized User Equilibrium (Watling, 2006), the travel time budget (Shao et al., 2006; Shao et al., 2006; Lo et al., 2006; Lam et al., 2008), the percentile User Equilibrium (Nie, 2011), the bi-criterion User Equilibrium proposed by Wang et al. (2004), the added-variability model (Ordóñez and Stier-Moses, 2010) and the mean-excess traffic equilibrium (Chen and Zhou, 2010; Chen et al., 2011b).

In this paper, we focus our attention on the mean-variance model (Jackson and Jucker, 1982), where the perceived utility for trip k and driver m is:

$$U_{km}^{od} = TC_k^{od} + \overline{TT}_k^{od} + VOR_m \times \sigma_k^{od}, \forall m \wedge \forall k \in \Omega^{od} \wedge \forall (o,d) \in \Xi \tag{5}$$

where VOR_m is the value of reliability for driver m. In the case where all drivers have the same preferences for the reliability of travel times, the term VOR_m reduces to $VOR \implies U_{km}^{od} = U_k^{od}$. The term TC_k^{od} represents the travel cost associated with each trip k. This travel cost can come from tolls, the fuel consumed during the trip, ticket costs, maintenance and insurance costs of the private car, to name a few examples.

The implementation of traffic assignment models in a dynamic context (i.e. with a traffic simulator that allows to determine travel times that account for dynamic effects such as shockwaves propagation and spillback effects) has significantly evolved since the initial works of Merchant and Nemhauser (1978a) and Merchant and Nemhauser (1978b). In the literature one can distinguish between two approaches to solve dynamic traffic assignment problems. The analytical approach (e.g. Wie et al., 2002; Szeto and Lo, 2006; Iryo, 2011; Corthout et al., 2012) is used to study the existence and uniqueness of the city network equilibrium. The simulation approach (e.g. Ben-Akiva et al., 2012; Mahmassani et al., 2013; Shafiei et al., 2018; Ameli et al., 2020) makes use of traffic simulators to determine time-dependent trip travel times that account for dynamic effects, such as congestion, shock-waves and spillback effects. In this paper, we focus our attention in this second approach. Drivers are assigned based on a quasi-static approximation, i.e. the total simulation period T is split into several time intervals δt where the network equilibrium is calculated. The trip flows are kept constant during each δt. The length of these time intervals can be adjusted to update the trip flows more frequently for cases when the demand suffers quick changes or when the traffic states change rapidly. We also refer the reader for the comprehensive review papers of Peeta and Ziliaskopoulos (2001) and Viti and Tampère (2010).

3. Methodological framework

In this section, we start by recalling the Regional Dynamic Traffic Assignment framework proposed by Batista and Leclercq (2019b) (Sect. 3.1). We then discuss the proposed extensions to incorporate bounded rational drivers with indifferent preferences and with preferences for more reliable travel times (Sect. 3.2).

3.1. Regional Dynamic Traffic Assignment R-DTA

The R-DTA proposed by Batista and Leclercq (2019b) includes several steps:

1. The definition of a set of trips in the city network.
2. The calculation of paths on the regional network based on the set of trips.

3. The characterization of the distributions of travel distances of the regional paths.
4. The determination of the travel times of the regional paths for performing the network loading.

The first step consists on defining a set of trips in the city network. One solution is to utilize real trajectories of drivers that are gathered from Global Positioning System (GPS) traces, i.e. using a data-driven method. However, the information about the full daily trip patterns is unknown, and only a partial set of real trips is available. The challenge here is to infer a level of confidence regarding how this partial set is representative of the full daily trip patterns. While this is still a question of research, in this paper we follow the idea proposed by Batista and Leclercq (2018) and Batista et al. (2019), to construct a set of virtual trips. The authors propose to randomly sample several origin and destination pairs of nodes in the city network, and then to determine the shortest-path in distance between each of them. Each virtual trip represents an individual driver traveling in the city network.

The next step consists in identifying the regional paths based on the set of virtual trips and on the definition of the city network partitioning. The regional paths are gathered by scaling-up these virtual trips following the sequence of regions they cross according to the definition of the city network partitioning (Batista and Leclercq, 2018), see Figure 2. For each regional Origin-Destination (OD) pair, the regional paths are ranked by their level of significance, i.e. the number of virtual trips each regional path has associated. Note that, regional paths can also be gathered directly from the daily trip patterns of drivers or from data analysis, to name two other examples. The most significant regional path of one OD pair is the one that has the largest number of virtual trips associated. We set the composition of the regional choice set, Ω^{OD}, for the most significant regional paths.

In the third step, we characterize the distributions of travel distances of the regional paths. Let L_{rp} be the trip length distribution of a generic regional path p in a generic region r. Batista et al. (2019) proposes a methodological framework to explicitly calculate these distributions, given the set of virtual trips and different levels of information from the regional network. The latter ranges from no prior information about the previous and next regions to be traveled by the virtual trips, to the related regional path. In this paper, we calculate the trip length distributions L_{rp} following the related regional path associated to the virtual trips. We refer the reader to Batista et al. (2019) for more details about the description of this methodological framework. Again, data-driven methods may also be used here to derive the trip length distributions of regional paths.

The fourth step consists on determining the travel times of regional paths, for performing the network loading. In regional networks the travel time of a regional path p is influenced by the empirical set of trip lengths $\{L_{rp}\}$ and the time varying speed-MFD set $v_r(n_r)$ of each region r that defines p. The travel time of a regional path p, TT_p^{OD}, is then calculated as:

$$TT_p^{OD} = \sum_{r \in X} \left(\frac{L_{rp}}{v_r(n_r)} \right) \delta_{rp}, \forall p \in \Omega^{OD} \wedge \forall (O, D) \in W \tag{6}$$

where W is the set of all regional OD pairs; and δ_{rp} is a binary variable that equals 1 if regional path p crosses region r, or 0 otherwise.

Batista and Leclercq (2019a) and Batista and Leclercq (2019b) target the User Equilibrium, considering different formulations of the utility function U_p^{OD}. The utility functions are determined based on a first order Taylor's expansion of the TT_p^{OD} equation (see Eq. 6) around the mean values of $\overline{L}_{rp}$ and $\overline{v}_r$.

For the Deterministic User Equilibrium (DUE), none of the terms are considered to be distributed. The utility function U_p^{OD} then becomes:

$$U_p^{OD} = \sum_{r \in X} \left(\frac{\overline{L}_{rp}}{\overline{v}_r} \right) \delta_{rp}, \forall p \in \Omega^{OD} \wedge \forall (O, D) \in W \tag{7}$$

While, for the Stochastic User Equilibrium (SUE), both L_{rp} and $v_r(n_r)$ are considered to be distributed. The utility function U_p^{OD} is then:

$$U_p^{OD} = \sum_{r \in X} \left(\frac{\overline{L}_{rp}}{\overline{v}_r} + \frac{L_{rp}}{\overline{v}_r} - \frac{\overline{L}_{rp} v_r}{\overline{v}_r^2} \right) \delta_{rp}, \forall p \in \Omega^{OD} \wedge \forall (O, D) \in W \tag{8}$$

In the classical DUE and SUE, drivers seek to minimize their own perceived travel times. The numerical scheme for determining these network equilibria are discussed in Batista and Leclercq (2019b), and summarized in Algorithm 1.

3.2. Extension of the R-DTA for bounded rational drivers

In this paper, we propose to extend the R-DTA framework proposed by Batista and Leclercq (2019a) and Batista and Leclercq (2019b), to account for bounded rational drivers with indifferent preferences as well as preferences for more travel time reliability.

We first focus on bounded rational drivers with indifferent preferences (Batista et al., 2018). For simplicity, we only focus on the travel time component, TT_p^{OD}, to define the utility function, U_p^{OD}, of a generic regional path p, i.e. $U_p^{OD} = TT_p^{OD}, \forall p \in \Omega^{OD} \wedge \forall (O,D) \in W$. Bounded rational drivers with indifferent preferences choose any regional path(s) that is/are perceived as *satisficing*, i.e. the one(s) that has/have the travel time(s) inferior to the aspiration level or that respect the condition $U_p^{OD} \leq AL^{OD}, \forall p \in \Omega^{OD} \wedge \forall (O,D) \in W$. The aspiration levels are calculated through the definition of the indifference band Δ^{OD} as defined in Eq. 4, but set at the regional OD level. The question now is how drivers choose among the *satisficing* regional paths. For this, we follow the idea proposed by Batista et al. (2018) where the demand of each regional OD pair is equally split over all *satisficing* regional paths. The network equilibrium corresponds to the Bounded Rational User Equilibrium (BR-UE).

We now focus on bounded rational drivers with preferences for more reliable travel times. To include the Value of Reliability in the R-DTA, we consider the mean-variance model (Jackson and Jucker, 1982). We then set the utility function defined by Eq. 5 to the regional OD level. Furthermore, for the sake of simplicity, we assume that all drivers sharing the same regional OD pair have similar preferences. The perceived utility of regional path p is expressed as:

$$U_p^{OD} = TC_p^{OD} + VOT_p E(TT_p^{OD}) + VOR_p Var(TT_p^{OD}), \forall p \in \Omega^{OD} \wedge \forall (O,D) \in W \tag{9}$$

where $E(TT_p^{OD})$ is the expected travel time; and $Var(TT_p^{OD})$ is the variance of the travel time distribution.

The expected travel time $E(TT_p^{OD})$ is calculated as:

$$E(TT_p^{OD}) = \sum_{r \in X} \left(\frac{\overline{L}_{rp}}{\overline{v}_r(n_r)} \right) \delta_{rp} \tag{10}$$

The variance $Var(TT_p^{OD})$ is calculated as:

$$Var(TT_p^{OD}) = \sum_{r \in X} \left(\frac{\overline{L}_{rp}}{\overline{v}_r(n_r)} \right)^2 \left(\frac{Var(L_{rp})}{\overline{L}_{rp}^2} + \frac{Var(v_r(n_r))}{\overline{v}_r^2(n_r)} - 2\frac{Cov(L_{rp}, v_r(n_r))}{\overline{L}_{rp}\overline{v}_r(n_r)} \right) \delta_{rp} \tag{11}$$

We refer the reader to Appendix A for the full derivation of Eq. 11.

In the same spirit as in the case of indifferent preferences, drivers choose any regional path(s) that is/are perceived as *satisficing* (i.e. $U_p^{OD} \leq AL^{OD}$). The difference is that the regional path utility U_p^{OD} is calculated by the mean-variance model defined in Eq. 9.

3.3. Numerical scheme and implementation algorithm

In this paper, we determine the regional network equilibrium using the classical Method of Successive Averages (MSA). The good convergence properties of the algorithm are guaranteed by the appropriate choice of the descent step α_j, where j is the descent iteration. In this paper, we choose $\alpha_j = \frac{1}{j}$ (see e.g. Polyak (1990); Liu et al. (2007); Taale (2008); Chen et al. (2011a) for different settings of α_j). Monte Carlo simulations (Sheffi, 1985) are used to account for the empirical distributions of trip lengths, L_{rp}, and the speed-MFD, $v_r(n_r)$, as in the same spirit of Batista and Leclercq (2019a) and Batista and Leclercq (2019b). The goal is to draw samples from the distributions L_{rp} and $v_r(n_r)$

and locally solve deterministic problems. At each descent step j of the MSA, the new regional path flows $Q_p^{OD,j+1}$ are updated as follows:

$$Q_p^{OD,j+1} = Q_p^{OD,j} + \eta_j\{Q_p^{OD,*} - Q_p^{OD,j}\}, \forall p \in \Omega^{OD} \wedge \forall (O,D) \in W \tag{12}$$

where $Q_p^{OD,j}$ represent the regional path flows at iteration j and $Q_p^{OD,*}, \forall (O,D) \in W$ represent the new temporary regional path flows. The question now is how to determine $Q_p^{OD,*}$. For the Deterministic and Stochastic User Equilibrium, drivers are assigned to the regional path with the lowest travel time, for each regional OD pair, based on an all-or-nothing principle. In the case of bounded rational drivers, they are assigned to the *satisficing* regional paths according to the assignment rules discussed in the previous section, for both cases. The term $Q_p^{OD,*}$ is then updated by averaging over all local choices of drivers.

The regional network equilibrium is achieved (Sbayti et al., 2007) when the relative Gap is inferior to a pre-defined tolerance tol and the number of violations $N(\lambda)$ is inferior to a pre-defined threshold Φ. We also set a maximum number of descent step iterations N_{max}. The number of violations represents the difference of the regional path flows between consecutive descent step iterations of the Method of Successive Averages. The relative Gap as defined by Sbayti et al. (2007) not only acts as a convergence criterion, but also as a quality indicator that tells how far the solution determined is from the *User Equilibrium* conditions. In case of the DUE, the MSA should convergence to a solution where $Gap \sim 0$. While, in the case of the SUE, the value of the Gap is larger than 0, however small. This happens because of the uncertainty associated with the trip length distributions L_{rp} as well as due to the evolution of the traffic conditions in the regions (i.e. $n_r(n_r)$ over time. In this paper, we utilize the definition of the Gap as introduced by Sbayti et al. (2007), for setting the convergence for both the DUE and SUE. The Gap is determined as:

$$Gap^{UE} = \frac{\sum_O \sum_D \sum_{p \in \Omega^{OD}} Q_p^{OD}(\overrightarrow{U}_p^{OD} - \min(\overrightarrow{U}^{OD}))}{\sum_O \sum_D Q^{OD} \min(\overrightarrow{U}^{OD}))} \tag{13}$$

where $\overrightarrow{U}_p^{OD}$ is a vector that contains all the values of the utility functions for all regional paths p that connect the regional OD pair.

In the case of the Bounded Rational User Equilibrium, we utilize the definition of the Gap as introduced by Batista et al. (2018). It is determined as:

$$Gap^{BR-UE} = \frac{\sum_O \sum_D \sum_{p \in \Omega^{OD}} Q_p^{OD} \cdot \max(\overrightarrow{U}^{OD} - AL^{OD}, 0)}{\sum_O \sum_D Q^{OD} \cdot AL^{OD}} \tag{14}$$

In this paper, we assign drivers based on a quasi-static approximation as function of the regional paths travel times, as described in Sect. 2.

Algorithm 1 summarizes the implementation of the numerical scheme for solving for the DUE, SUE or BR-UE by means of the Method of Successive Averages and utilizing a quasi-static approximation.

4. Model implementation

In this section, we start by introducing the city network and demand scenarios in Sect. 4.1. We then investigate how the preferences for more reliable travel times of bounded rational drivers influences the traffic dynamics in the regions (Sect. 4.2). In Sect. 4.3, we investigate how the level of bounded rational drivers influences the NO_x and CO_2 emissions at the regional network level.

4.1. Definition of the case study

The test network depicted in Figure 3 (a) and includes the 3^{rd} and 6^{th} districts of Lyon and the city of Villeurbanne (L63V network) in France. The network has 3127 nodes and 3363 links and is divided into seven regions. The

Algorithm 1: Pseudo-code algorithm used to determine the User Equilibrium or Bounded Rational User Equilibrium on regional networks.

Input the regional choice set $\Omega^{OD}, \forall (O,D) \in W$, the set of trip lengths $L_{rp}, \forall p \in \Psi \wedge \forall r \in X$, demand scenario, simulation duration T and the convergence tolerances tol, ϕ and N_{max}. Input also the indifference band Δ^{OD} if one targets the BR-UE.

for *i=1 to* $\frac{T}{\delta t}$ **do**

  Initialize $j = 1$, $\alpha_{j=1} = 1$ and the temporary path flows $Q_p^{OD,j+1}$.

  if *i=1* **then**

    Initialize the path flows $Q_p^{OD,j=1}, \forall p \in \Omega^{OD} \wedge \forall (O,D) \in W$. Also initialize the aspiration levels AL^{OD} (Eq. 4), if one targets the BR-UE.

    Perform an initial network loading.

  else

    Initialize $Q_p^{OD,j=1}, \forall p \in \Omega^{OD} \wedge \forall (O,D) \in W$ from the path flows at equilibrium from the previous period $i-1$.

  end

  while $Gap \geq tol$ **and/or** $N(\lambda) \geq \Phi$ **and** $j \leq N_{max}$ **do**

    Set $Q_p^{OD,j} = Q_p^{OD,j+1}, \forall p \in \Omega^{OD} \wedge \forall (O,D) \in W$.

    For all regions $r \in X$, calculate the average mean speed $\overline{v}_r$ based on v_r.

    if *DUE* **then**

      Determine the regional path utilities according to Eq. 7.

      Assign drivers based on all-or-nothing procedure to the regional path(s) with the minimal U_p^{OD}, and update $Q_p^{OD,*}, \forall p \in \Omega^{OD} \wedge \forall (O,D) \in W$.

    end

    if *SUE* **then**

      Perform Monte Carlo simulations to account for the distributions of L_{rp} and $v_r(n_r)$, and determine the determine the regional path utility U_p^{OD} (Eq. 8) for each realization or draw.

      Assign drivers based on all-or-nothing principle to the path with the minimal utility U_p^{OD}, for each realization.

      Determine $Q_p^{OD,*}$ by averaging the drivers choices over all Monte Carlo realizations.

    end

    if *BR-UE* **then**

      if *Indifferent preferences* **then**

        Determine the regional path utilities U_p^{OD} according to Eq. 7.

      end

      if *Strict preferences* **then**

        Determine the regional path utilities U_p^{OD} according to Eq. 9.

      end

      Update $Q_p^{OD,*}$ by equally splitting the demand over all *satisficing paths*, i.e. paths that respect the condition $U_p^{OD} \leq AL^{OD}$.

      Update the aspiration levels $AL^{OD}, \forall (O,D) \in W$ according to Eq. 4.

    end

    Update the path flows $Q_p^{OD,j+1}$ based on Eq. 12.

    Run the MFD-based model (either the accumulation- or trip-based MFD model).

    Update $v_r, \forall r \in X$, based on the traffic states resulting from the MFD-based model.

    Determine the Gap according to Eq. 13 (if DUE or SUE) or Eq. 14 (if BR-UE) and the number of violations $N(\lambda)$.

    Update $\alpha_j = \frac{1}{j}$.

    Set $j = j + 1$.

  end

end

MFD functions are shown in Figure 3 (b), and have been fitted considering microscopic simulations from Symuvia (Leclercq, 2007). The simulated data is fitted using a bi-parabolic shape.

The calibration of the trip lengths distributions and the calculation of the regional paths are based on a set of 3.000.000 virtual trips (Batista and Leclercq, 2018; Batista et al., 2019). The regional paths are ranked according to their level of significance.

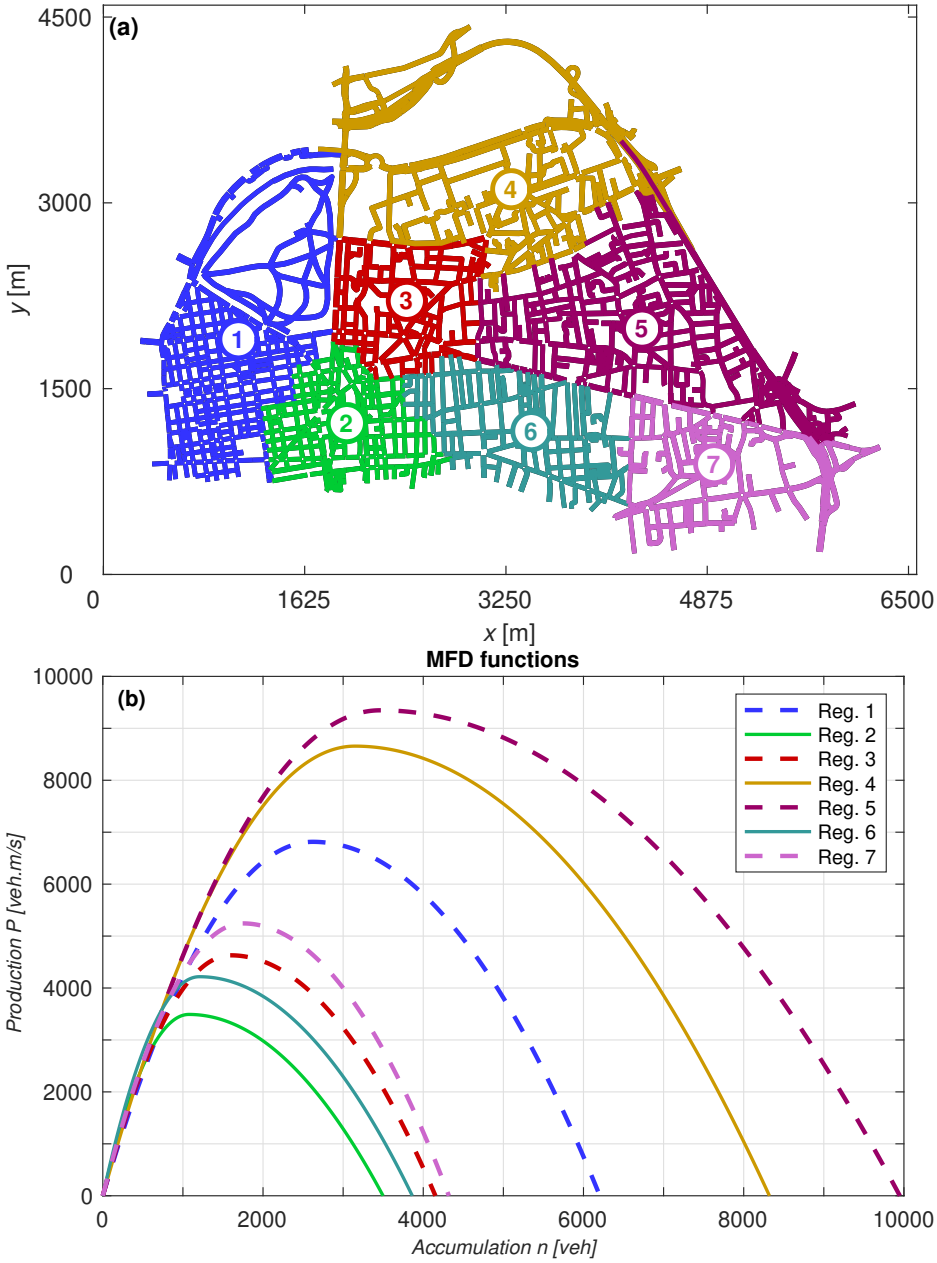

Figure 3: (a) Villeurbanne and the 3^{rd} and 6^{th} districts of Lyon (France) traffic network, divided into seven regions. (b) Calibrated MFD function of each region.

In this paper, we consider two distinct scenarios:

- *Scenario 1:* The first scenario is calibrated to investigate the role of the VOR in the traffic dynamics in the regions (Sect. 4.2). It is composed by two OD pairs: 2-4; and 5-1. The regional choice sets Ω^{OD} contain the

two most significant regional paths for each OD pair. Table 1 lists the regional paths as well as the calculated average trip lengths ($\overline{L}$) and standard deviations (σ_L) of the trip lengths distributions. Figure 4 (a) depicts the demand levels for this scenario.

Table 1: Average and standard deviations of the trip lengths distributions ($\overline{L} \pm \sigma_L$) (m) calculated for the four regional paths in each region. The total average trip length $\overline{L}$ for each regional path is also listed.

Regional path	Region					$\overline{L}$
	1	2	3	4	5	
2-3-4	~	652 ± 312	1092 ± 218	1097 ± 760	~	2841
2-1-3-4	431 ± 181	512 ± 308	780 ± 214	1877 ± 1313	~	3599
5-3-2-1	901 ± 494	460 ± 58	797 ± 24	~	1289 ± 598	3447
5-3-1	900 ± 437	~	1398 ± 309	~	919 ± 461	3217

In this first scenario, we fix the indifference band Δ^{OD} to 1 and set three *VOR* values: $0, 1 \times 10^{-3}$, and 10.

- *Scenario 2:* The second scenario is more complex and is calibrated to investigate how the bounded rational behavior of drivers influences the emission levels of NO_x and CO_2 at the regional network level (Sect. 4.3). The latter includes bounded rational drivers with indifferent preferences and drivers with preferences for more reliable travel times. This scenario is composed by eight OD pairs: 1-4; 2-5; 4-7; 5-1; 5-2; 6-2; 6-5; and 7-1. The regional choice sets Ω^{OD} includes the three most significant regional paths for each OD pair. This yields a total of 24 regional paths. Figure 4 (b) depicts the demand levels for the eight OD pairs of this scenario. For the bounded rational drivers with indifferent preferences, we set three values of Δ^{OD}: 0, 1 and 100. While, for the bounded rational drivers with preferences for more reliable travel times, we fix $\Delta^{OD} = 1$ and set three values for VOR: $0, 1 \times 10^{-3}$ and 1.

The total simulation periods are $T = 8000$ seconds for *Scenario 1*, and $T = 15000$ seconds for *Scenario 2*. We assume a quasi-static approximation for determining the network equilibrium, and the total simulation period T is split into several time intervals of amplitude $\delta t = 200$ seconds. The network equilibrium is calculated for each interval δ, during which the regional path flow distributions are maintained constant. The classical MSA algorithm is used to calculate the regional network equilibrium. We set the MSA convergence tolerances to $tol = 10^{-2}$, $\Phi = 0$ and $N_{max} = 250$. For the Monte Carlo simulations, we consider 10000 samples from each L_{rp} and $v_r(n_r)$ distributions. The traffic dynamics is simulated using an accumulation-based MFD traffic model (Daganzo, 2007; Geroliminis and Daganzo, 2008), and the implementation details follow Mariotte et al. (2017). However, we stress out that the proposed methodological framework in this paper is also valid for the application of the trip-based MFD model to mimic the traffic dynamics in the regions.

4.2. *Influence of travel time reliability on the traffic dynamics in the regions*

In this section, we investigate the influence of the choices of bounded rational drivers with preferences for more reliable travel times on the traffic dynamics in the regions. Figure 5 shows the evolution of the traffic dynamics in regions 1 to 5 as well as the evolution of the regional path flows for $p = \{234\}$, $p = \{5321\}$ and $p = \{531\}$. Regions 6 and 7 are omitted since they are not crossed by any of the previous regional paths.

We start by analyzing the regional path flows at equilibrium. The quasi-static assignment approximation plays an important role on the influence of the regional speed $\overline{v}_r(n_r)$ on the calculation of the network equilibrium. Batista and Leclercq (2019a) and Batista and Leclercq (2019b) show that the regional speed $\overline{v}_r(n_r)$ has a more significative influence during the charging and discharging period of the regions. However, the variance of the mean speed distribution $v_r(n_r)$, i. e. $Var(v_r(n_r))$, is generally smaller than the variance of the trip length distribution L_{rp}, i. e. $Var(L_{rp})$. This means that:

$$\sum_{r \in X} \left(\frac{Var(L_{rp})}{\overline{L}_{rp}^2} \right) \delta_{rp} \gg \sum_{r \in X} \left(\frac{Var(v_r(n_r))}{\overline{v}_r^2(n_r)} - 2 \frac{Cov(L_{rp}, v_r(n_r))}{\overline{L}_{rp} \overline{v}_r(n_r)} \right) \delta_{rp} \tag{15}$$

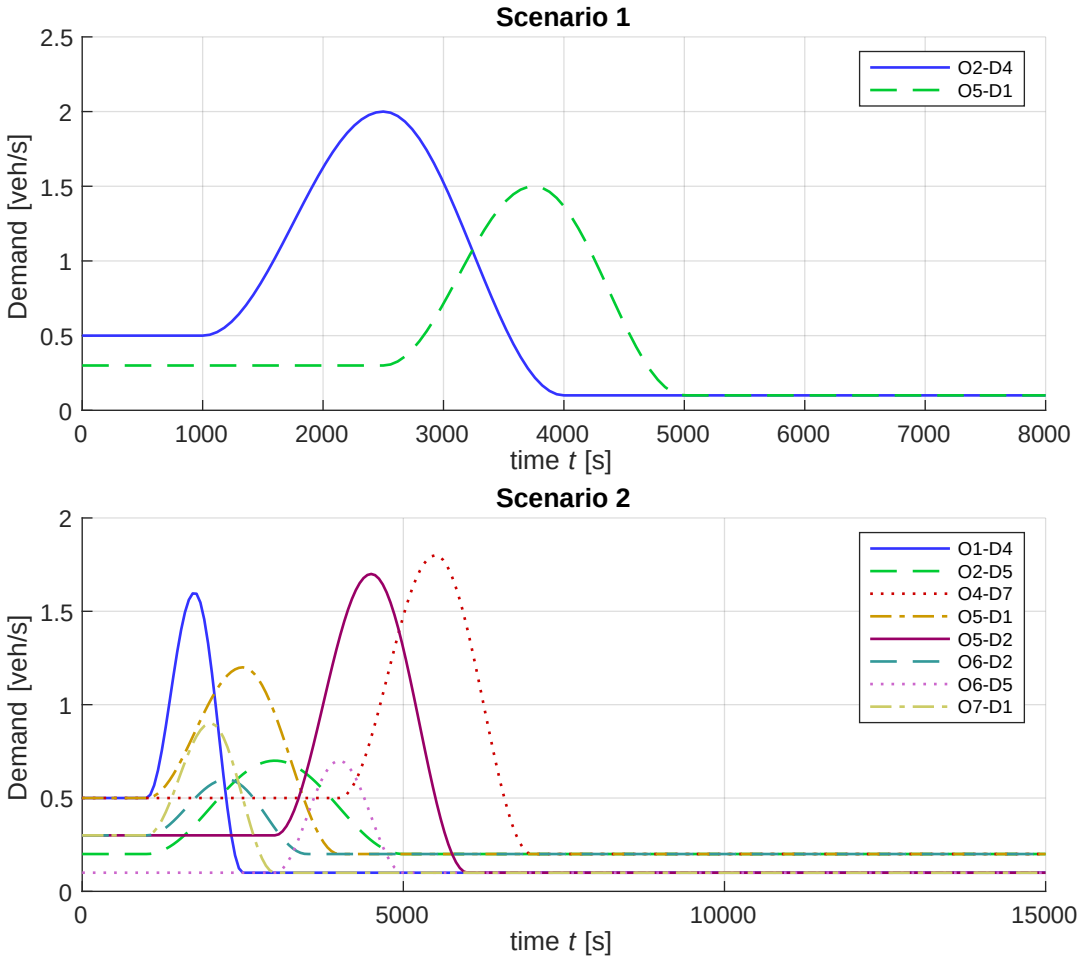

Figure 4: Demand levels for *Scenario 1* (panel a) and *Scenario 2* (panel b).

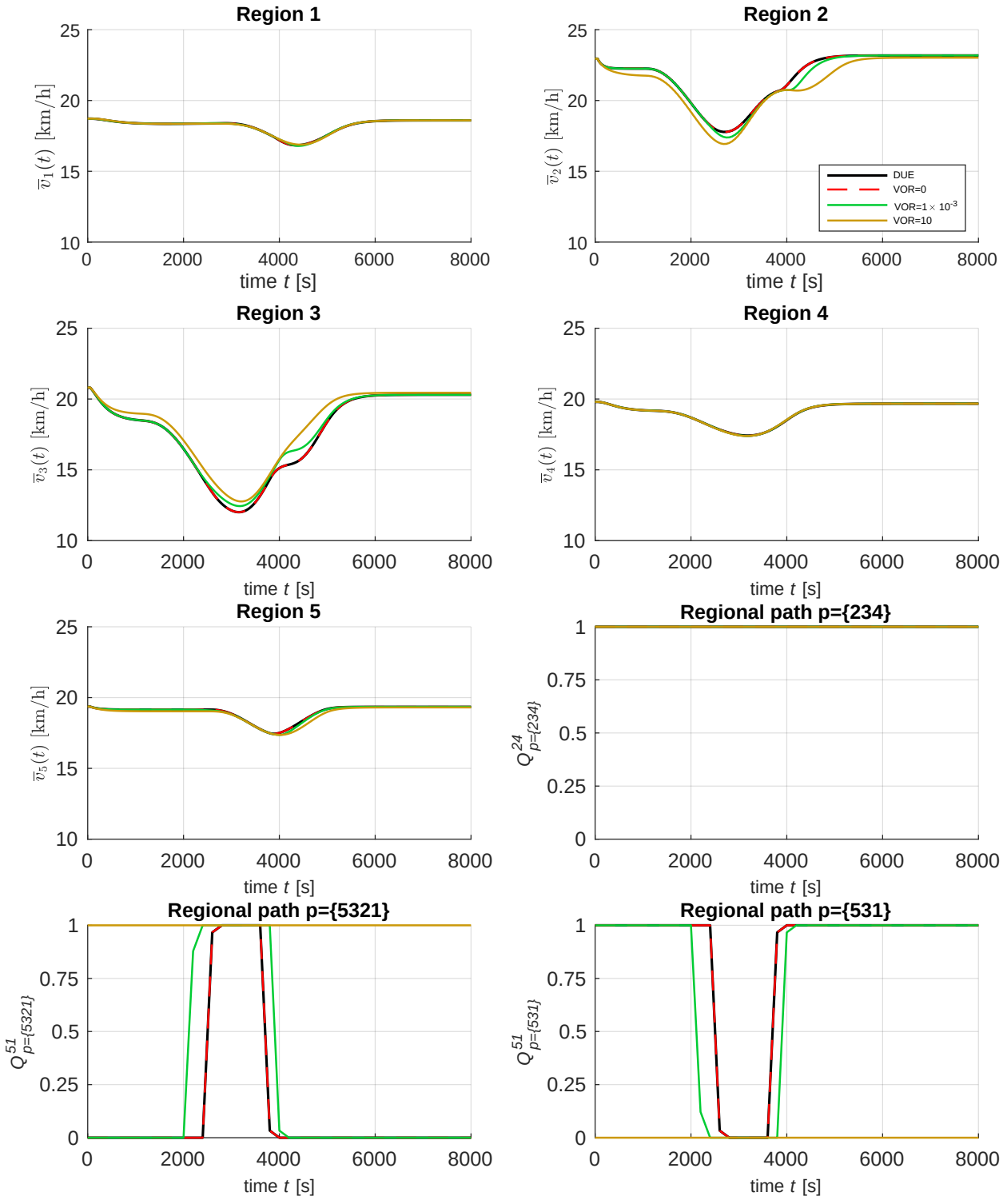

Figure 5: Evolution of the regional mean speed $v(t)$ for Scenario 1. The results are shown for the DUE and different settings of the VOR. The indifference band Δ^{OD} is fixed to 1 and five values of VOR are considered: $0, 1 \times 10^{-3}$ and 10. The evolution of the regional path flows Q_p^{OD} for $p = \{234\}$, $p = \{5321\}$ and $p = \{531\}$ are also shown.

Outside the congestion periods and offset in the regions, we also have that: $Var(v_r(n_r)) = 0 \implies Cov(L_{rp}, v_r(n_r)) = 0$. From Eq. 9 to Eq. 11, we can further simplify the regional path U_p^{OD}. In this case:

$$U_p^{OD} = \sum_{r \in X} \left(\frac{\overline{L}_{rp}}{\overline{v}_r(n_r)} + VOR \frac{Var(L_{rp})}{\overline{v}_r^2} \right) \delta_{rp}, \forall p \in \Omega^{OD} \wedge \forall (O, D) \in W \tag{16}$$

We emphasize that when VOR is set to 0 in Eq. 16, the regional network equilibrium reduces to the Deterministic User Equilibrium. This is also confirmed by the results shown in Figure 5. We observe that by setting $VOR = 0$, we obtain similar evolution trends of the regional path flows as well as similar traffic dynamics in the regions, compared to the DUE. We can also observe from Figure 5, that drivers always choose the regional path $p = \{234\}$ over the whole simulation period, since its travel time is more reliable. The speeds $\overline{v}_2$, $\overline{v}_3$ and $\overline{v}_4$ influence equally the utilities of both regional paths $p = \{234\}$ and $p = \{2134\}$. The differences between the regional path utilities arise from the trip length distributions. From Table 1, we observe that both the average trip lengths as well as the standard deviations are approximately equal for regions 2 and 3 and for both regional paths $p = \{234\}$ and $p = \{2134\}$. The difference lies in region 4. The average trip length and standard deviations assigned for region 4, are much larger for the regional path $p = \{2134\}$ than for $p = \{234\}$. The travel time is then more reliable for $p = \{234\}$. For the OD pair 5-1, we observe that drivers initially choose regional path $p = \{531\}$. At $\sim$ 2000 seconds, region 3 becomes congested because there are more vehicles traveling on regional path $p = \{234\}$ (see Figure 4 (a)). This leads to a switch of the regional paths chosen by drivers traveling on the OD 5-1. The average trip length and standard deviations assigned for region 3, is much larger for regional path $p = \{531\}$ than for $p = \{5321\}$ (see Table 1). Then, as the vehicles' accumulation in region 3 increases, the travel time of $p = \{5321\}$ becomes more reliable and drivers switch to this path. An inverse trend is observed when region 3 is discharging. We also notice that as VOR increases, the term $\sum_{r \in X} \frac{Var(L_{rp})}{\overline{v}_r^2} \delta_{rp}$ becomes more important in the regional path utility defined in Eq. 16. In the case of OD 5-1, the increase of VOR penalizes more the utility of the regional path $p = \{531\}$ as its average trip length and standard deviation of the trip length distribution for region 3, are much larger than the ones calculated for regional path $p = \{5321\}$. The travel time reliability of $p = \{531\}$ increases as VOR also does, leading drivers to switch to this regional path.

We now briefly analyze the traffic dynamics depicted in Figure 5 for the five regions. We start by region 2, that is the origin one for the regional path $p = \{234\}$. Between $\sim$ 1500 and 3500 seconds, we observe a decrease in the mean speed $\overline{v}_2$ due to an increase of the demand traveling on regional path $p = \{234\}$. After completing their travels in regions 2, vehicles cross to region 3 and then 4, leading to a decrease in the mean speeds $\overline{v}_3$ and $\overline{v}_4$, between $\sim$ 1800 and 4000 and $\sim$ 2000 and 4000 seconds, respectively. We also observe that as VOR increases, the vehicles' speed reduces in region 2 while it increases in region 3. The increase of VOR leads drivers to switch from regional path $p = \{531\}$ to $p = \{5321\}$, as previously explained, reducing the mean speeds in these regions. This routing of vehicles reduces the accumulation in region 3, slightly increasing its mean speed $\overline{v}_3$. An opposite trend is verified in region 2. We also observe two interesting trends in the mean speed profiles of regions 2 and 3, between $\sim$ 4000 and 6000 seconds. These profiles are originated by vehicles traveling in the OD pair 5-1. The average trip length calculated for region 3 and regional path $p = \{531\}$ is 1398 meters (see Table 1). While, for regional path $p = \{5321\}$ is 797 meters. A larger trip length means that a region is a potential bottleneck for the regional path. Due to the homogeneous speed assumption of the MFD, for larger trip lengths drivers require more time to complete their travels in the region. This increases the accumulation and decreases the region mean speed. In the case of region 3, vehicles switch to regional path $p = \{5321\}$ as VOR increases. The lower trip length allows vehicles to complete their trips faster, reducing the accumulation and increasing the mean speed. In the case of region 2, the mean speed decreases for a longer period as there are more vehicles traveling on regional path $p = \{5321\}$.

4.3. Estimation of emissions of CO_2 and NO_x

Road traffic is a major source in the air quality degradation in large urban areas. The greenhouse effect is one of the main environmental issues. It is mainly caused by CO_2 emissions. These emissions are originated by the fuel consumption of motorized vehicles. On the other hand, the NO_x emissions represent a serious issue for public health. They are mainly related with accelerations and decelerations of vehicles. This is why when the mean speed is low we observe a significant increase of the emission function since such speed is related to congested traffic conditions

with frequent stop-and-go phases. In this section, we investigate how drivers' rationality (i.e. DUE, SUE and BR-UE) influences the CO_2 and NO_x emissions at the regional network level. We estimate these concentrations using the COPERT IV model (Ntziachristos et al., 2009). Note that, COPERT IV is an aggregated model, i.e. applicable to a region or zone of a city network, that takes as an input an average speed and total travel distance. For each mean speed value, the model already includes the driving cycles that account for accelerations and decelerations of vehicles. The calculation of the Emission Factors of CO_2 (EF_{CO_2}) and NO_x (EF_{NO_x}) are based on reference emission data recorded for a mean speed profile of private cars. We further assume a homogeneous fleet over the whole network. Figure 6 depicts the emission laws for the Emission Factors of CO_2 and NO_x.

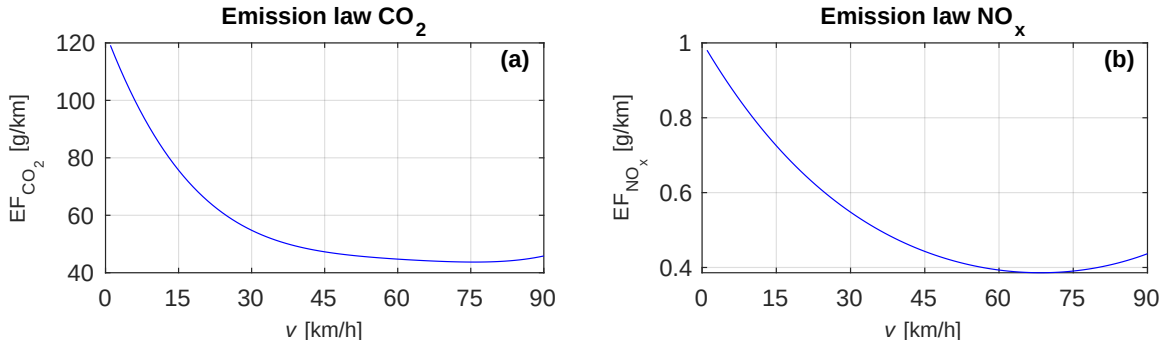

Figure 6: Emission laws for CO_2 (panel a) and NO_x (panel b).

Figure 7 depicts the evolution of the vehicles' mean speeds $\overline{v}_r(n_r)$ for the DUE, SUE and the three settings of Δ^{OD} for the bounded rational users with indifferent preferences. Figure 8 shows similar results, but for the bounded rational drivers with preferences for more reliable travel times and for the three settings of VOR. Figure 9 shows the relative differences θ between the different settings of the bounded rational models and the DUE and SUE. The relative differences θ are calculated as:

$$\theta = \frac{EF_x^{w,z} - EF_x^y}{EF_x^y} \times 100, x = \{CO_2, NO_x\} \wedge y = \{DUE, SUE\} \tag{17}$$

where w represents the value of Δ^{OD}; and z represents the VOR.

We first focus on the analysis of the results for bounded rational drivers with indifferent preferences. One can observe in Figure 7 that for $\Delta^{OD} = 0$, the evolution of the mean speed $\overline{v}_r(n_r)$ is similar to the SUE. In fact, when $\Delta^{OD} = 0$, drivers seek to minimize their own travel times and the bounded rational stochastic user equilibrium reduces to the classical SUE. As Δ^{OD} increases, drivers are able to choose regional paths with longer travel times, and that also correspond to regional paths with larger travel distances. A longer travel distance inside a region means a potential bottleneck, since drivers need more time to complete their trips. We recall that drivers travel at the same speed inside the regions because of the homogeneous speed assumption of the MFD model. This increases the accumulation of vehicles for a longer period of time, decreasing the mean speed in the regions. This can be observed in Figure 7, for example, for regions 3, 4 and 5. As $\Delta^{OD} \rightarrow \infty$, the regional path flows tend to $1/K$, where K is the number of regional paths listed in Ω^{OD}. This represents the drivers indifference for their regional path choice when all paths are perceived as *satisficing*, explaining why $\overline{v}_r(n_r)$ decreases in some regions as Δ^{OD} increases. Figure 9 shows that as Δ^{OD} increases, the concentrations of CO_2 and NO_x also do with respect to the benchmark models.

The indifferent preferences lead drivers to choose any of the *satisficing* regional paths, meaning that for larger Δ^{OD} more drivers will choose regional paths with longer travel distances. This increases the total travel distance of all drivers, explaining the increase of the emission factors of CO_2 and NO_x as observed in Figure 9. We observe that the complete indifference of drivers for their regional path choice, i.e. $\Delta^{OD} = 100$, leads to an increase of $\sim 20\%$ of CO_2 and NO_x emissions compared to the benchmark DUE and SUE models, i.e. perfect rational drivers. The observed trend for CO_2 and NO_x emissions is directly related with the increase of the travel distances, as previously explained. For larger Δ^{OD}, drivers choose longer regional paths, requiring more time to complete their trips in the regions. This

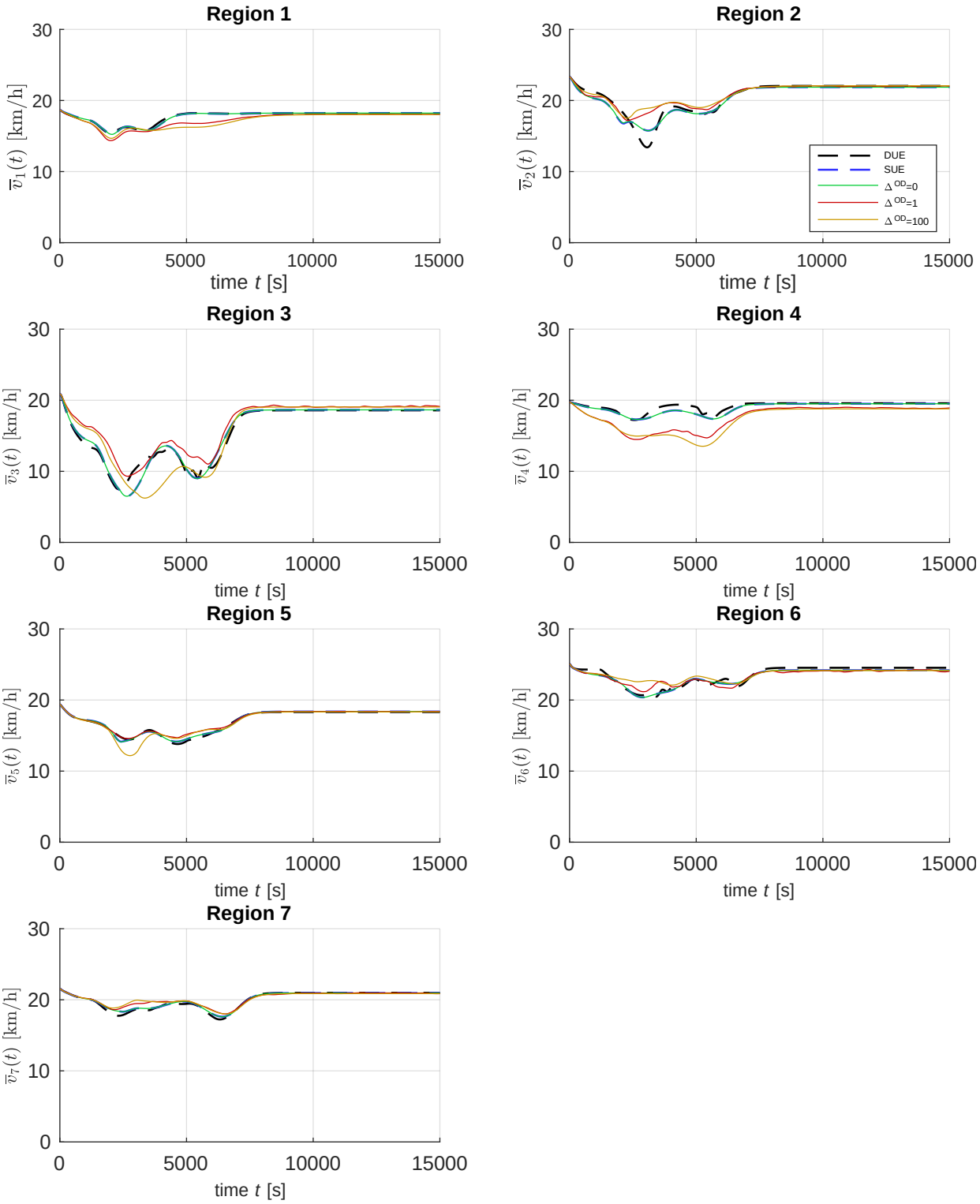

Figure 7: Evolution of the mean speed $\overline{v}_r(n_r)$ for the seven regions and for the DUE, SUE, and bounded rational drivers with indifferent preferences. The indifference band values Δ^{OD} are set to 0, 1 and 100.

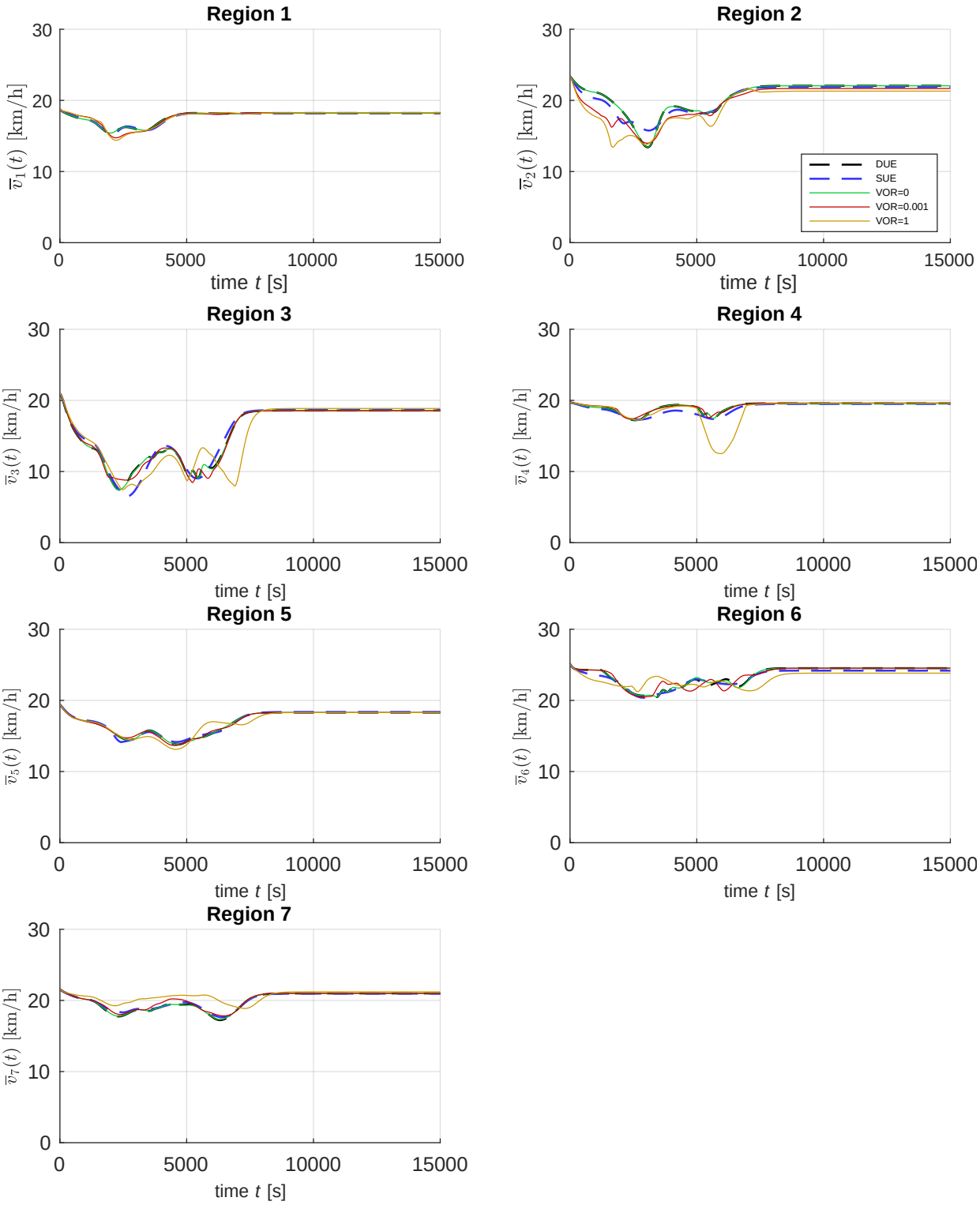

Figure 8: Same as in Figure 7, but for the bounded rational drivers with preferences for more reliable travel times. The indifference band Δ^{OD} is set to 1. The VOR values are set to $0, 1 \times 10^{-3}$ and 10.

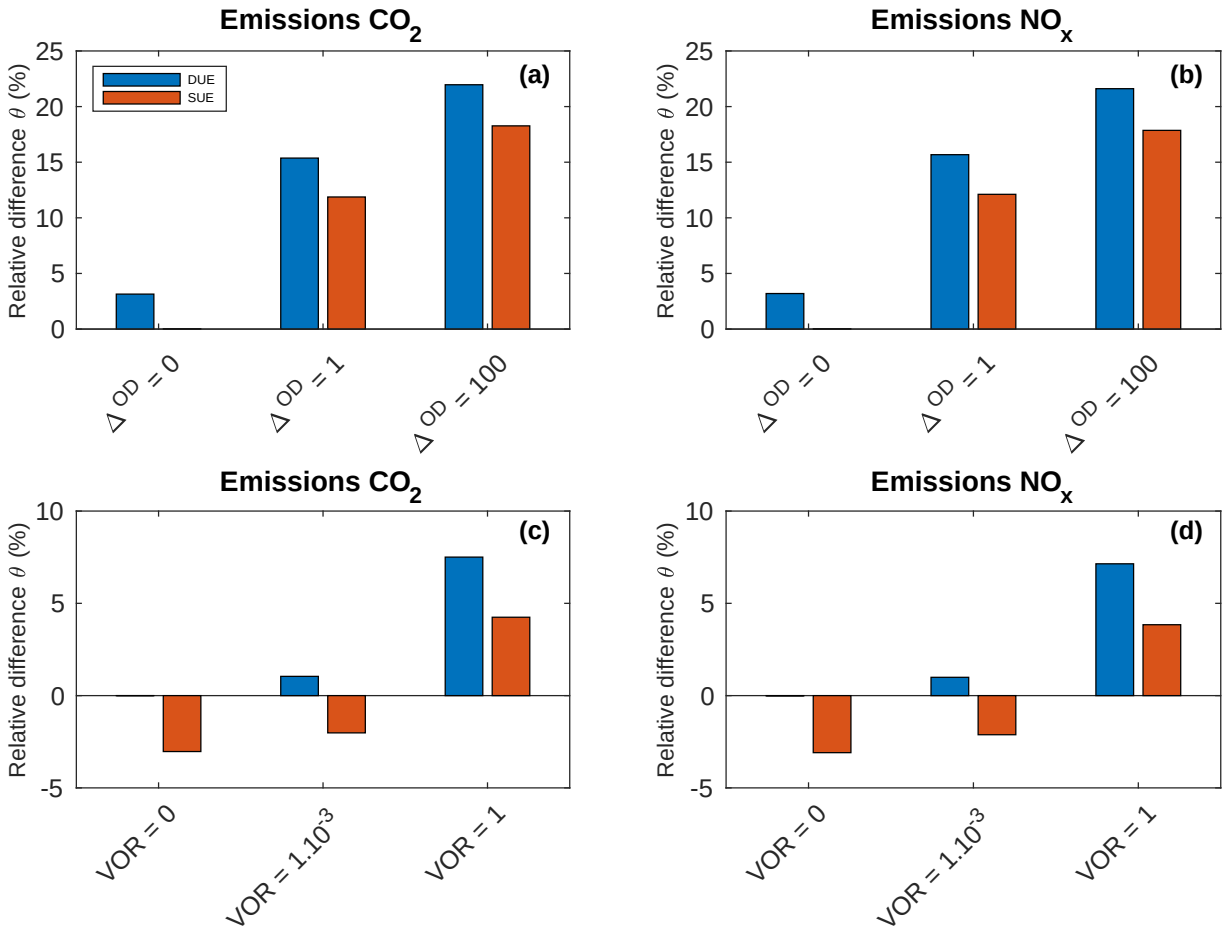

Figure 9: Relative differences between the estimated total emissions of CO_2 and NO_x (in kg/km) between the different settings of the bounded rational drivers with indifferent preferences (panels a and b) and with preferences for more reliable travel times (panels c and d), and the DUE and SUE. The orange bars represent the relative differences with respect to the DUE, while the blue ones are with respect to the SUE.

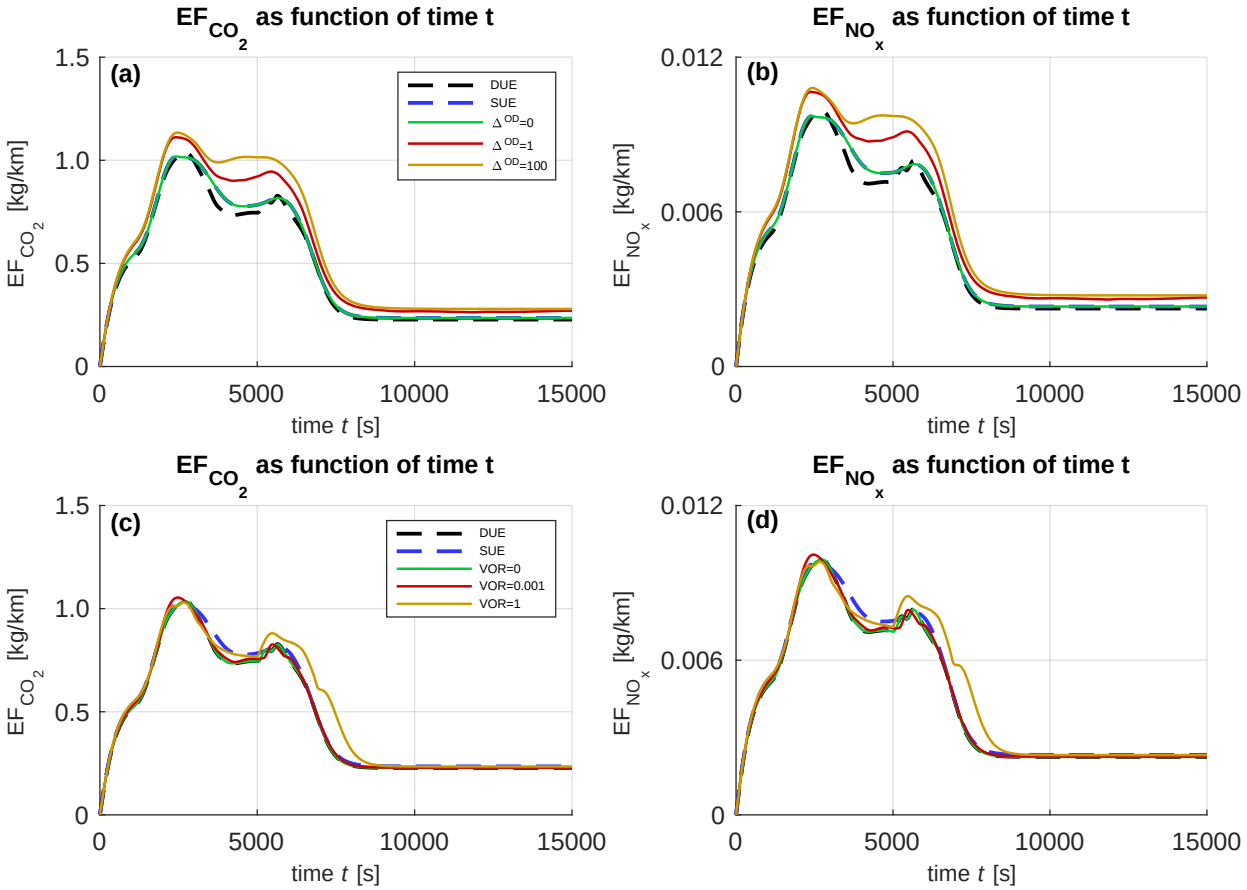

Figure 10: Temporal evolution of EF_{CO_2} and EF_{NO_x} for the whole network. The results are depicted for the different settings of the bounded rational models, where drivers have indifferent preferences (panel a and b) as well as preferences for reliable travel times (panel c and d), and the benchmark DUE and SUE. The emission factors are determined for time periods of 10 seconds.

increases both the length and congestion levels in the regions, leading to a larger reduction of the mean speed v_r, and consequently to more frequent stop-and-go phases for larger Δ^{OD} values during the charging periods of the regions. Figure 10 (a-b) depicts the temporal evolution of CO_2 and NO_x emissions, for drivers with indifferent preferences. We observe an increase of the emissions, between $\sim$ 1000 and 2000 seconds, which corresponds to the moment when the demand in the network also increases (see Figure 4 (b)). This leads to an increase of the accumulation, reducing the traveling mean speed in the regions and increasing the frequency of stop-and-go phases. An opposite trend is observed during the discharging of the regions between $\sim$ 6000 and 7000 seconds, reducing the CO_2 and NO_x emissions. The travel distances then directly influence the CO_2 and NO_x emissions.

We now focus on the analysis of the results for bounded rational drivers with preferences for more reliable travel times. We set the indifference band Δ^{OD} to 1, and vary VOR^{OD}. For $VOR = 0$, drivers do not have a preference for more reliable travel times and only the expected travel time $E(TT_p^{OD})$ matters in their choices. The network equilibrium is reduced to the Bounded Rational Deterministic User Equilibrium that is calculated for $\Delta^{OD} = 1$. The drivers' preferences for more reliable travel times increase with VOR. As VOR increases, drivers switch to paths that have more reliable travel times. Regional paths with the more reliable travel times are not necessarily the ones that have the shortest travel distances, as depicted in Figure 11. The latter can be analyzed in two different perspectives. In one hand, for an average path travel distance $\overline{L}_p$ of $\sim$ 3.5 kms, the standard deviation σ_L ranges from $\sim$ 1 to 2 kms. On the other hand, for a standard deviation value σ_L around $\sim$ 0.95 kms, the average travel distances can range from $\sim$ 2 to 4 kms. So, in a first approximation (see Eq. 16), the switch of drivers to paths with more reliable travel depends on the balance between the average travel distance and the variance of the trip length distributions of the regional paths.

In *Scenario 2*, there are some examples of the latter. In the regional choice set Ω^{14}, the regional path $p = \{134\}$ has the shortest travel distance but its trip length distribution has the largest variance. While, regional path $p = \{1234\}$ has a slightly larger trip length than $p = \{134\}$, but the variance of the trip length distribution is much lower. Another example is the regional choice set Ω^{25}, where the regional path $p = \{235\}$ has an average travel distance of 2725 meters and standard deviation 923 meters. While, the regional path $p = \{2345\}$ has an average travel distance of 3075 meters and standard deviation of 861 meters. Since drivers switch to regional paths with more reliable travel times, which for several OD pairs also have longer travel distances, they need more time to complete their trips in the regions. The congestion then lasts longer and the mean speed in the regions decreases. This can clearly be observed in Figure 8, for regions 3, 4 and 6, between the period $\sim$ 1000 and $\sim$ 6000 seconds. On the other hand, the total distance traveled by drivers increases as VOR also does, as inspected from Figure 11. For $VOR = 0$, the network equilibrium reduces to the classical DUE, and then $\theta \sim 0\%$, see Figure 9 (c-d). Drivers choose paths with more reliable travel times as VOR increases, which do not necessarily correspond to the shortest paths in distance as previously discussed. This induces an increase of the CO_2 and NO_x emissions in the whole network. The larger total distance traveled by drivers, for $VOR = 1$ compared to $VOR = 0$, increases the congestion level in the regions and then the stop-and-go phases. An opposite trend is observed during the discharging period of the regions, decreasing the CO_2 and NO_x emissions, see Figure 10 (c-d) between ~6000 and 7000 seconds. One can also observe in Figure 9 that the relative differences θ are much smaller when drivers have preferences for more reliable travel times than when they are completely indifferent for their path choices. The largest relative differences for both NO_x and CO_2 are $\sim 6\%$ when compared to the DUE, and $\sim 3\%$ when compared to the SUE. In the case of indifferent preferences, θ is $\sim 15\%$ when compared to the DUE, and $\sim 12\%$ when compared to the SUE. Note that here, we analyze the θ values for $\Delta^{OD} = 1$ for both kinds of preferences. This difference is explained by the fact that the total traveled distance by drivers is larger in the case of indifferent preferences. This result sheds light on the importance of properly accounting for drivers' behavior for the path choices in the estimation of CO_2 and NO_x emissions at the network level.

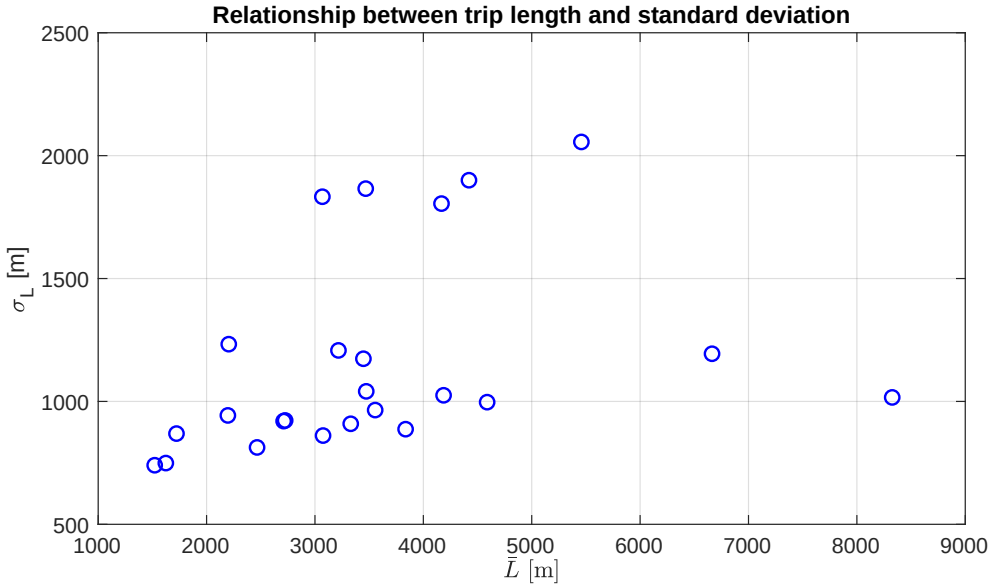

Figure 11: Relationship between the standard deviation σ_L and average travel distance L_p of all 24 regional paths of *Scenario 2*.

5. Conclusions

In this paper, we propose an extension of the R-DTA framework discussed by Batista and Leclercq (2019a) and Batista and Leclercq (2019b) to account for bounded rational drivers with indifferent preferences as well as drivers with preferences for more reliable travel times. We show that: (i) it is important to properly account for more realistic

drivers' rationality as it changes the estimation of emissions; and (ii) it is clear that making the system closer to the User Equilibrium (when compared to more realistic network equilibria, in terms of the drivers' behavior) would be beneficial for the environment. These results enhance the importance of developing efficient travel time information systems, e.g. Advanced Travel Information Systems (ATIS), such that drivers favor best choices knowing is reliable. As future research directions, we envision the experimental calibration and validation our framework using real observations.

6. Discussion

This paper discusses an extension of the R-DTA framework to account for more realistic drivers' behavior towards their regional path choice, by relaxing the principle of the *User Equilibrium*. We then shed light on potential applications for estimating the network-wide emissions of CO_2 and NO_x. Macroscopic emissions models can indeed be directly plugged on the traffic simulation outputs. The resulting emission calculations take then into account the regional urban dynamics resulting from the spread of congestion inline with the drivers routing behavior.

The main advantage of our framework for this kind of application lies in the computational efficiency and the low calibration requirements to set up the simulation scenario. The other alternative would be microscopic simulations if we still want to consider traffic dynamics. It comes at considerable costs in terms of network implementation, model calibration, and even more critical the demand estimation. As microscopic simulations resort to the real road network, multiple origins and destinations should be considered, which complexifies the origin-destination flows estimation particularly for large city networks. This explains why emission calculations at the city level are still often performed in practice using inventory methods or simple static approximations, which completely disregard the effects of congestion. The introduction of the concept of regional networks, let us focus on an aggregated vision of the whole system, which simplifies both the calibration and the demand estimation. It makes this framework easily scalable for different demand patterns. Preparing the simulation scenarios is also much lighter when compared to classical microscopic approaches at a large city scale.

Another main advantage of this methodological framework is the considerable simplification of the network equilibrium calculations compared to more classical approaches. The characterization of the regional network lengths adds an extra step, but it can be done one for all before simulating all different scenarios. As the regional network is represented by a graph with few edges and nodes by definition, all paths discovery and cost assessments are swift and the convergence to equilibrium much faster, simply because the problem is made much smaller. The classical DTA modules for city networks work with the full vision of the road network. It brings several challenges. The first lies in identifying plausible trips to travel by drivers (path discovery step). For large metropolitan areas, the number of origin-destination pairs as well as trips to consider is infinite, and the DTA model quickly becomes untraceable. On the contrary, the R-DTA framework starts from partitioning the city network into a limited number of regions (typically ten regions or less for large metropolitan areas). The origin-destination pairs of nodes in the city network are aggregated to Origin-Destination pairs of regions. Since the number of regions is low, this drastically reduces the number of plausible paths. Such a scale-up process of the information reduces the computational burden required by the R-DTA compared to the classical link-based assignment models and microscopic simulations. Ameli et al. (2020) discusses the computational complexity of classical link-based DTA models on city networks. The authors targeted the network equilibrium on the same city network utilized in this study and depicted in Figure 3 (a), considering 94 origin and 227 destination nodes. The city network was loaded with 47,341 travelers. The authors show that using classical methods, like the Method of Successive Averages for determining the equilibrium on this medium-sized city network, takes about a week of computational time. Even with advanced meta-heuristics approaches based on the Simulated Annealing and the Genetic Algorithms, the authors were unable to reduce the computational times below 36 hours. This drastically reduces the number of scenarios that can be explored in practice. The R-DTA framework we are investigating here determines the equilibrium solution on the same network in a matter of minutes. Such a feature is priceless for decision-making in practice, as it highlights the stakeholders with the benefits of multiple options.

Nevertheless, the low computational effort required by the R-DTA and aggregated traffic models based on the MFD has some drawbacks. The aggregation step from the city to the regional networks leads to loss of information, mostly in the description of distance traveled. In a nutshell, the city network description provides an accurate description of every trip distances. Such trips are aggregated into a single path at the regional level as long as they come and end into the same regions. Regional paths are characterized by a mean distance value and the standard deviation of the

related distribution. As far as emission calculations are concerned, the related bias should still be precisely quantified. However, as vehicular emissions are proportional to the distance travel, we can claim that the bias between the sum of distance and a mean value applied to all vehicles should be low when the total number of vehicles is high (law of large numbers). Another potential bias is if the trip distributions appear significantly different between equilibria derived at different scales (city or regional ones). This question would require significant research efforts that are out of the scope of the current study, being a potential future research direction. Note that recent efforts about experimental validation of MFD models show promising results about the reproduction of overall traffic dynamics Mariotte et al. (2020). It is not entirely conclusive about the specific question of the vehicle distribution over the network, but traffic dynamics would not be accurate if this would have been wrong.

About the emission calculation itself, the use of macroscopic models, like COPERT, looks relevant in our framework as the traffic simulation outputs fit the model input requirements, i.e. mean speeds and travel distances estimation. Such models have been proven accurate at large-scale as long as multiple trips are considered together (Lejri and Leclercq, 2020). One can claim that more accurate results can be obtained when coupling microscopic traffic and emission models. It would require that the speed evolution calculated by the traffic models be very accurate, which has not been proven yet. Microscopic emission laws are sensitive to acceleration and deceleration values. To our best knowledge, no microscopic traffic simulator has demonstrated high accuracy to this respect as they have been mainly designed to reproduce traffic flows and not kinematics.

Finally, we would like to stress that our framework has been designed to ensure consistency between the local trips in the city network and the regional paths (Batista and Leclercq, 2018), as well as the travel distances. It means that our model can adequately capture at the regional scale travel distances, which is one of the main elements for calculating traffic-related emission. As discussed in Mariotte et al. (2020), multi-regional systems are sufficient to reproduce the mean-speed dynamics inside each region. It means that our multi-regional framework directly determines the two main variables for emission calculations (mean speeds and travel distances) at the macroscopic level while considering traffic dynamics. The purpose of this paper is to show that our framework fulfills the requirements for emission calculations and can then be used to compare the drivers' rationality for their chosen path.

Acknowledgements

This project is supported by the European Research Council (ERC) under the European Union's Horizon 2020 research and innovation program (grant agreement No 646592 - MAGnUM project).

Appendices

A. Mathematical derivation of the variance of the travel time distribution

In this section, we discuss the derivation of the mathematical expression utilized to characterize the variance of the distributions of travel times TT_p^{OD} (see Eq. 11). From the definition of the variance, we have that:

$$Var(TT_p^{OD}) = E\{[TT_p^{OD} - E(TT_p^{OD})]^2\} \tag{A.1}$$

We start by recalling the reader that the travel time TT_p^{OD} (see Eq. 6) of a regional paths is determined by means of a first order Taylor's expansion around the mean values of $\overline{L}_{rp}$ and $\overline{v}_r$ (Batista and Leclercq, 2019b). We then obtain that:

$$TT_p^{OD} = \sum_{r \in X} \left(\frac{\overline{L}_{rp}}{\overline{v}_r} + \frac{1}{\overline{v}_r}(L_{rp} - \overline{L}_{rp}) - \frac{\overline{L}_{rp}}{\overline{v}_r^2}(v_r - \overline{v}_r) \right) \delta_{rp}, \forall p \in \Omega^{OD} \wedge \forall (O, D) \in W \tag{A.2}$$

By plugging Eq. A.2 and Eq. 10 into Eq. A.1, we have that:

$$Var(TT_p^{OD}) = E\left\{ \sum_{r \in X} \left[\frac{\overline{L}_{rp}}{\overline{v}_r(n_r)} + \frac{1}{\overline{v}_r(n_r)}(L_{rp} - \overline{L}_{rp}) - \frac{\overline{L}_{rp}}{\overline{v}_r^2(n_r)}(v_r(n_r) - \overline{v}_r(n_r)) - \frac{\overline{L}_{rp}}{\overline{v}_r(n_r)} \right]^2 \delta_{rp} \right\} \tag{A.3}$$

From Eq. A.3 we reorganize the terms:

$$Var(TT_p^{OD}) = E\left\{ \sum_{r \in X} \left[\frac{1}{\overline{v}_r(n_r)}(L_{rp} - \overline{L}_{rp}) - \frac{\overline{L}_{rp}}{\overline{v}_r^2(n_r)}(v_r(n_r) - \overline{v}_r(n_r)) \right]^2 \delta_{rp} \right\} \tag{A.4}$$

We now develop the quadratic term in Eq. A.4, and do some arithmetic calculations to re-organize the terms:

$$Var(TT_p^{OD}) = E\left\{ \sum_{r \in X} \left[\frac{1}{\overline{v}_r^2(n_r)}(L_{rp} - \overline{L}_{rp})^2 + \frac{\overline{L}_{rp}^2}{\overline{v}_r^4(n_r)}(v_r(n_r) - \overline{v}_r(n_r))^2 - 2\frac{\overline{L}_{rp}}{\overline{v}_r^3(n_r)}(L_{rp} - \overline{L}_{rp})(v_r(n_r) - \overline{v}_r(n_r)) \right] \delta_{rp} \right\} \tag{A.5}$$

We determine the expected value $E(.)$ of the right term in Eq. A.5, and we obtain that:

$$Var(TT_p^{OD}) = \sum_{r \in X} \left\{ \frac{1}{\overline{v}_r^2(n_r)} E((L_{rp} - \overline{L}_{rp})^2) + \frac{\overline{L}_{rp}^2}{\overline{v}_r^4(n_r)} E((v_r(n_r) - \overline{v}_r(n_r))^2) - 2\frac{\overline{L}_{rp}}{\overline{v}_r^3(n_r)} E((L_{rp} - \overline{L}_{rp})(v_r(n_r) - \overline{v}_r(n_r))) \right\} \delta_{rp} \tag{A.6}$$

Note that, in Eq. A.6, $E(L_{rp}) = \overline{L}_{rp}$ and $E(v_r(n_r)) = \overline{v}_r(n_r)$. The terms $E((L_{rp} - \overline{L}_{rp})^2)$, $E((v_r(n_r) - \overline{v}_r(n_r))^2)$ and $E((L_{rp} - \overline{L}_{rp})(v_r(n_r) - \overline{v}_r(n_r)))$ in Eq. A.6, represent the variances the distributions of travel distances L_{rp}, distributions of mean speeds $v_r(n_r)$ and the covariance between these two distributions, respectively. We then substitute these terms in Eq. A.6 and we have that:

$$Var(TT_p^{OD}) = \sum_{r \in X} \left\{ \frac{1}{\overline{v}_r^2(n_r)} Var(L_{rp}) + \frac{\overline{L}_{rp}^2}{\overline{v}_r^4(n_r)} Var(v_r(n_r)) - 2\frac{\overline{L}_{rp}}{\overline{v}_r^3(n_r)} Cov(L_{rp}, v_r(n_r)) \right\} \delta_{rp} \tag{A.7}$$

From Eq. A.7, we isolate the term $\left(\frac{\overline{L}_{rp}}{\overline{v}_r(n_r)} \right)^2$. We then obtain our final expression (also present on Eq. 11) for the variance of TT_p^{OD}:

$$Var(TT_p^{OD}) = \sum_{r \in X} \left(\frac{\overline{L}_{rp}}{\overline{v}_r(n_r)} \right)^2 \left(\frac{Var(L_{rp})}{\overline{L}_{rp}^2} + \frac{Var(v_r(n_r))}{\overline{v}_r^2(n_r)} - 2\frac{Cov(L_{rp}, v_r(n_r))}{\overline{L}_{rp}\overline{v}_r(n_r)} \right) \delta_{rp} \tag{A.8}$$

References

Ambühl, L., Loder, A., Zheng, N., Axhausen, K.W., Menendez, M., 2019. Approximative network partitioning for mfds from stationary sensor data. Transportation Research Record 2673, 94103. URL: https://dx.doi.org/10.1177/0361198119843264.

Ameli, M., Lebacque, J.P., Leclercq, L., 2020. Flow exchanges in multi-reservoir systems with spillbacks. Simulation Modelling Practice and Theory 99, 101995. URL: dx.doi.org/10.1016/j.simpat.2019.101995, doi:10.1016/j.simpat.2019.101995.

Arnott, R., 2013. A bathtub model of downtown traffic congestion. Journal of Urban Economics 76, 110–121. URL: https://dx.doi.org/10.1016/j.jue.2013.01.001, doi:10.1016/j.jue.2013.01.001.

Azevedo, J., Santos Costa, M., Silvestre Madeira, J., Vieira Martins, E., 1993. An algorithm for the ranking of shortest paths. European Journal of Operational Research 69, 97–106. URL: https://dx.doi.org/10.1016/0377-2217(93)90095-5, doi:10.1016/0377-2217(93)90095-5.

Batista, S.F.A., Leclercq, L., 2018. Introduction of multi-regional mfd-based models with route choices: the definition of regional paths, in: PLURIS 2018 - 8th LUSO-BRAZILIAN CONGRESS for Urban, Regional, Integrated and Sustainable Planning, Coimbra, Portugal.

Batista, S.F.A., Leclercq, L., 2019a. A dynamic traffic assignment framework for mfd multi-regional models, in: 98th Annual Meeting Transportation Research Board, Washington DC, USA.

Batista, S.F.A., Leclercq, L., 2019b. Regional dynamic traffic assignment framework for mfd multi-regions models. Transportation Science 53, 1563–1590. URL: https://dx.doi.org/10.1287/trsc.2019.0921, doi:10.1287/trsc.2019.0921.

Batista, S.F.A., Leclercq, L., Geroliminis, N., 2019. Estimation of regional trip length distributions for the calibration of the aggregated network traffic models. Transportation Research Part B: Methodological 122, 192–217. URL: https://dx.doi.org/10.1016/j.trb.2019.02.009, doi:10.1016/j.trb.2019.02.009.

Batista, S.F.A., Zhao, C.L., Leclercq, L., 2018. Effects of users bounded rationality on a traffic network performance: A simulation study. Journal of Advanced Transportation Article ID 9876598, 20. URL: https://doi.org/10.1155/2018/9876598, doi:10.1155/2018/9876598.

Bekhor, S., Prashker, J.N., 2001. Stochastic user equilibrium formulation for the generalized nested logit model. Transportation Research Record 1752, 84–90. URL: https://dx.doi.org/10.3141/1752-12, doi:10.3141/1752-12.

Ben-Akiva, M., Bergman, M.J., Daly, A., Ramaswamy, V., 1984. Modeling interurban route choice behaviour, in: Proceedings of the 9th International Symposium on Transportation and Traffic Theory, Utrecht, The Netherlands.

Ben-Akiva, M., Bierlaire, M., 1999. Handbook of Transportation Science. Springer US, Boston, MA. chapter Discrete Choice Methods and their Applications to Short Term Travel Decisions. pp. 5–33. URL: http://dx.doi.org/10.1007/978-1-4615-5203-1_2, doi:10.1007/978-1-4615-5203-1_2.

Ben-Akiva, M., Gao, S., W.Z., Wen, Y., 2012. A dynamic traffic assignment model for highly congested urban networks. Transportation Research Part C: Emerging Technologies 24, 62–82. URL: https://dx.doi.org/10.1016/j.trc.2012.02.006, doi:10.1016/j.trc.2012.02.006.

Bovy, P.H.L., Bekhor, S., Prato, C.G., 2008. The factor of revised path size: an alternative derivation. Transportation Research Record 2076, 132–140. URL: https://dx.doi.org/10.3141/2076-15, doi:10.3141/2076-15.

Casadei, G., Bertrand, V., Gouin, B., Canudas-de-Wit, C., 2018. Aggregation and travel time calculation over large scale traffic networks: An empiric study on the grenoble city. Transportation Research Part C: Emerging Technologies 95, 713–730. URL: https://dx.doi.org/10.1016/j.trc.2018.07.033, doi:10.1016/j.trc.2018.07.033.

Cascetta, E., Nuzzolo, A., Russo, F., Vitetta, A., 1996. A modified logit route choice model overcoming path overlapping problems: specification and some calibration results for interurban networks, in: Proceedings of the 13th International Symposium on Transportation and Traffic Theory, Lyon, France. pp. 697–711.

Chen, A., Pravinvongvuth, S., Xu, X., Ryu, S., Chootinan, P., 2012. Examining the scaling effect and overlapping problem in logit-based stochastic user equilibrium models. Transportation Research Part A 46, 1343–1358. URL: http://dx.doi.org/10.1016/j.tra.2012.04.003, doi:10.1016/j.tra.2012.04.003.

Chen, A., Xiangdong, X., Ryu, S., Zhou, Z., 2011a. A self-adaptive armijo stepsize strategy with application to traffic assignment models and algorithms. Transportmetrica A: Transport Science 9, 695–712. URL: http://dx.doi.org/10.1080/18128602.2011.653999, doi:10.1080/18128602.2011.653999.

Chen, A., Zhou, Z., 2010. The α-reliable mean-excess traffic equilibrium model with stochastic travel times. Transportation Research Part B: Methodological 44, 493 – 513. URL: http://dx.doi.org/10.1016/j.trb.2009.11.003, doi:10.1016/j.trb.2009.11.003.

Chen, A., Zhou, Z., Lam, W.H.K., 2011b. Modeling stochastic perception error in the mean-excess traffic equilibrium model. Transportation Research Part B: Methodological 45, 1619 – 1640. URL: http://dx.doi.org/10.1016/j.trb.2011.05.028, doi:10.1016/j.trb.2011.05.028.

Chorus, C., 2012a. Logsums for utility-maximizers and regret-minimizers, and their relation with desirability and satisfaction. Transportation Research Part A: Policy and Practice 46, 1003–1012. URL: http://dx.doi.org/10.1016/j.tra.2012.04.008, doi:10.1016/j.tra.2012.04.008.

Chorus, C., 2012b. Random regret minimization: An overview of model properties and empirical evidence. Transport Reviews 32, 75–92. URL: http://dx.doi.org/10.1080/01441647.2011.609947, doi:10.1080/01441647.2011.609947.

Chorus, C., 2014. A generalized random regret minimization model. Transportation Research Part B: Methodological 68, 224–238. URL: http://dx.doi.org/10.1016/j.trb.2014.06.009, doi:10.1016/j.trb.2014.06.009.

Corthout, R., Flötteröd, G., Viti, F., Tampère, C.M.J., 2012. Non-unique flows in macroscopic first-order intersection models. Transportation Research Part B: Methodological 46, 343–359. URL: http://dx.doi.org/10.1016/j.trb.2011.10.011, doi:10.1016/j.trb.2011.10.011.

Dafermos, S.C., 1972. The traffic assignment problem for multiclass-user transportation networks. Transportation Science 6, 73–87. URL: https://dx.doi.org/10.1287/trsc.6.1.73, doi:10.1287/trsc.6.1.73.

Dafermos, S.C., 1980. Traffic equilibrium and variational inequalities. Transportation Science 14, 42–54. URL: https://dx.doi.org/10.1287/trsc.14.1.42, doi:10.1287/trsc.14.1.42.

Dafermos, S.C., 1982. The general multimodal network equilibrium problem with elastic demand. Networks 12, 52–72. URL: https://dx.doi.org/10.1002/net.3230120105, doi:10.1002/net.3230120105.

Daganzo, C., 2007. Urban gridlock: Macroscopic modeling and mitigation approaches. Transportation Research Part B: Methodological 41, 49–62. URL: https://dx.doi.org/10.1016/j.trb.2006.03.001, doi:10.1016/j.trb.2006.03.001.

Daganzo, C., Sheffi, Y., 1977. On stochastic models of traffic assignment. Transportation Science 11, 253–274. URL: https://dx.doi.org/10.1287/trsc.11.3.253, doi:10.1287/trsc.11.3.253.

Daganzo, C.F., 1982. Unconstrained extremal formulation of some transportation equilibrium problems. Transportation Science , 332–360URL: https://dx.doi.org/10.1287/trsc.16.3.332, doi:10.1287/trsc.16.3.332.

de la Barra, T., Perez, B., Anez, J., 1993. Multidimensional path search and assignment, in: Proceedings of the 21st PTRC Summer Annual Meeting, Manchester, England.

Di, X., He, X., Guo, X., Liu, H.X., 2014. Braess paradox under the boundedly rational user equilibria. Transportation Research Part B 67, 86–108.

URL: https://dx.doi.org/10.1016/j.trb.2014.04.005, doi:10.1016/j.trb.2014.04.005.
Di, X., Liu, H., Pang, J., Ban, X., 2013. Boundedly rational user equilibria (brue): mathematical formulation and solution sets. Transportation Research Part B 57, 300–313. URL: https://dx.doi.org/10.1016/j.trb.2013.06.008, doi:10.1016/j.trb.2013.06.008.
Di, X., Liu, H.X., 2016. Boundedly rational route choice behavior: A review of models and methodologies. Transportation Research Part B: Methodological 85, 142–179. URL: https://dx.doi.org/10.1016/j.trb.2016.01.002, doi:10.1016/j.trb.2016.01.002.
Dial, R., 1971. A probabilistic multipath traffic assignment model which obviates path enumeration. Transportation Research , 83–113URL: https://dx.doi.org/10.1016/0041-1647(71)90012-8, doi:10.1016/0041-1647(71)90012-8.
Flötteröd, G., Bierlaire, 2013. Metropolis-hastings sampling of paths. Transportation Research Part B 48, 53–66. URL: https://dx.doi.org/10.1016/j.trb.2012.11.002, doi:10.1016/j.trb.2012.11.002.
Fosgerau, M., 2013. A link based network route choice model with unrestricted choice set. Transportation Research Part B: Methodological 56, 70–80. URL: https://dx.doi.org/10.1016/j.trb.2013.07.012, doi:10.1016/j.trb.2013.07.012.
Fosgerau, M., 2015. Congestion in the bathtub. Economics of Transportation 4, 241–255. URL: https://dx.doi.org/10.1016/j.ecotra.2015.08.001, doi:10.1016/j.ecotra.2015.08.001.
Frejinger, E., Bierlaire, M., Ben-Akiva, M., 2009. Sampling of alternatives for route choice modelling. Transportation Research Part B 43, 984–994. URL: https://dx.doi.org/10.1016/j.trb.2009.03.001, doi:10.1016/j.trb.2009.03.001.
Geroliminis, N., Daganzo, C., 2008. Existence of urban-scale macroscopic fundamental diagrams: Some experimental findings. Transportation Research Part B: Methodological 42, 759–770. URL: https://dx.doi.org/10.1016/j.trb.2008.02.002, doi:10.1016/j.trb.2008.02.002.
Iryo, T., 2011. Multiple equilibria in a dynamic traffic network. Transportation Research Part B: Methodological 45, 867–879. URL: https://dx.doi.org/10.1016/j.trb.2011.02.010, doi:10.1016/j.trb.2011.02.010.
Jackson, W.B., Jucker, J.V., 1982. An empirical study of travel time variability and travel choice behavior. Transportation Science 16, 460–475. URL: https://dx.doi.org/10.1287/trsc.16.4.460, doi:10.1287/trsc.16.4.460.
Kazagli, E., Bierlaire, M., Flötteröd, G., 2016. Revisiting the route choice problem: A modeling framework based on mental representations. Journal of Choice Modelling 19, 1–23. URL: https://dx.doi.org/10.1016/j.jocm.2016.06.001, doi:10.1016/j.jocm.2016.06.001.
Knight, F.H., 1924. Some fallacies in the interpretation of social cost. The Quarterly Journal of Economics 38. URL: https://dx.doi.org/10.2307/1884592, doi:10.2307/1884592.
Lam, W.H., Shao, H., Sumalee, A., 2008. Modeling impacts of adverse weather conditions on a road network with uncertainties in demand and supply. Transportation Research Part B: Methodological 42, 890 – 910. URL: https://dx.doi.org/10.1016/j.trb.2008.02.004, doi:10.1016/j.trb.2008.02.004.
Lamotte, R., Geroliminis, N., 2016. The morning commute in urban areas: Insights from theory and simulation, in: Transportation Research Board 95^{th} Annual Meeting., pp. 16–2003.
Leclercq, L., 2007. Hybrid approaches to the solutions of the "lighthill-whitham-richards" model. Transportation Research Part B: Methodological 41, 701–709. URL: https://dx.doi.org/10.1016/j.trb.2006.11.004, doi:10.1016/j.trb.2006.11.004.
Leclercq, L., Sénécat, A., Mariotte, G., 2017. Dynamic macroscopic simulation of on-street parking search: A trip-based approach. Transportation Research Part B: Methodological 101, 268–282. URL: https://dx.doi.org/10.1016/j.trb.2017.04.004, doi:10.1016/j.trb.2017.04.004.
Lejri, D., Leclercq, L., 2020. Are average speed emission functions scale-free? Atmospheric Environment 224, 117324. URL: https://dx.doi.org/10.1016/j.atmosenv.2020.117324, doi:10.1016/j.atmosenv.2020.117324.
Li, M., Huang, H.J., 2016. A regret theory-based route choice model. Transportmetrica A: Transportation Science 13, 250–272. URL: https://dx.doi.org/10.1080/23249935.2016.1252445, doi:10.1080/23249935.2016.1252445.
Liu, H.X., He, X., He, B., 2007. Method of successive weighted averages (mswa) and self-regulated averaging schemes for solving stochastic user equilibrium problem. Networks and Spatial Economics 9, 485–503. URL: https://dx.doi.org/10.1007/s11067-007-9023-x, doi:10.1007/s11067-007-9023-x.
Lo, H.K., Luo, X., Siu, B.W.Y., 2006. Degradable transport network: Travel time budget of travelers with heterogeneous risk aversion. Transportation Research Part B: Methodological 40, 792–806. URL: https://dx.doi.org/10.1016/j.trb.2005.10.003, doi:10.1016/j.trb.2005.10.003.
Lopez, C., Leclercq, L., Krishnakumari, P., Chiabaut, N., van Lint, H., 2017. Revealing the day-to-day regularity of urban congestion patterns with 3d speed maps. Scientific Reports 7, 1–11. URL: https://dx.doi.org/10.1038/s41598-017-14237-8, doi:10.1038/s41598-017-14237-8.
Mahmassani, H., Saberi, M., Zockaie, A., 2013. Urban network gridlock: Theory, characteristics, and dynamics. Transportation Research Part C: Emerging Technologies 36, 480–497. URL: https://dx.doi.org/10.1016/j.trc.2013.07.002, doi:10.1016/j.trc.2013.07.002.
Mahmassani, H.S., Chang, G.L., 1987. On boundedly rational user equilibrium in transportation systems. Transportation Science 21, 89–99. URL: https://dx.doi.org/10.1287/trsc.21.2.89, doi:10.1287/trsc.21.2.89.
Mariotte, G., Leclercq, L., 2019. Flow exchanges in multi-reservoir systems with spillbacks. Transportation Research Part B: Methodological 122, 327 – 349. URL: http://www.sciencedirect.com/science/article/pii/S019126151731175X, doi:10.1016/j.trb.2019.02.014.
Mariotte, G., Leclercq, L., Batista, S., Krug, J., Paipuri, M., 2020. Calibration and validation of multi-reservoir mfd models: A case study in lyon. Transportation Research Part B: Methodological 136, 62 – 86. URL: http://www.sciencedirect.com/science/article/pii/S0191261519306769, doi:https://doi.org/10.1016/j.trb.2020.03.006.
Mariotte, G., Leclercq, L., Laval, J.A., 2017. Macroscopic urban dynamics: Analytical and numerical comparisons of existing models. Transportation Research Part B 101, 245–267. URL: https://dx.doi.org/10.1016/j.trb.2017.04.002, doi:10.1016/j.trb.2017.04.002.
McFadden, D., 1978. Spatial Interaction Theory and Planning Models. MIT Press, Cambridge, MA. chapter Modelling the choice of residential location. pp. 75–96.
Merchant, D.K., Nemhauser, G.L., 1978a. A model and an algorithm for the dynamic traffic assignment problems. Transportation Science 12,

183–199. URL: https://doi.org/10.1287/trsc.12.3.183, doi:10.1287/trsc.12.3.183.
Merchant, D.K., Nemhauser, G.L., 1978b. Optimality conditions for a dynamic traffic assignment model. Transportation Science 12, 200–207. URL: https://doi.org/10.1287/trsc.12.3.200, doi:10.1287/trsc.12.3.200.
Nie, Y.M., 2011. Multi-class percentile user equilibrium with flow-dependent stochasticity. Transportation Research Part B: Methodological 45, 1641 – 1659. URL: https://dx.doi.org/10.1016/j.trb.2011.06.001, doi:10.1016/j.trb.2011.06.001.
Nielsen, O.A., 2000. A stochastic transit assignment model considering differences in passengers utility functions. Transportation Research Part B 34, 377–402. URL: https://dx.doi.org/10.1016/S0191-2615(99)00029-6, doi:10.1016/S0191-2615(99)00029-6.
Nielsen, O.A., Daly, A., Frederiksen, R.D., 2002. A stochastic route choice model for car travellers in the copenhagen region. Networks and Spatial Economics 2, 327–346. URL: https://dx.doi.org/10.1023/A:102089542, doi:10.1023/A:102089542.
Ntziachristos, L., Gkatzoflias, D., Kouridis, C., Samaras, Z., 2009. Copert: A european road transport emission inventory model, in: Athanasiadis, I.N., Rizzoli, A.E., Mitkas, P.A., Gómez, J.M. (Eds.), Information Technologies in Environmental Engineering, Springer Berlin Heidelberg, Berlin, Heidelberg. pp. 491–504. URL: https://doi.org/10.1007/978-3-540-88351-7_37, doi:10.1007/978-3-540-88351-7_37.
Ordóñez, F., Stier-Moses, N.E., 2010. Wardrop equilibria with risk-averse users. Transportation Science 44, 63–86. URL: https://dx.doi.org/10.1287/trsc.1090.0292, doi:10.1287/trsc.1090.0292.
Peeta, S., Ziliaskopoulos, A.K., 2001. Foundations of dynamic traffic assignment: The past, the present and the future. Networks and Spatial Economics 1, 233–265. URL: https://dx.doi.org/10.1023/A:1012827724856, doi:10.1023/A:1012827724856.
Polyak, B., 1990. New method of stochastic approximation type. Automation and Remote Control 51, 937–946.
Prashker, J.N., Bekhor, S., 1998. Investigation of stochastic network loading procedures. Transportation Research Record 1645, 94–102. URL: https://dx.doi.org/10.3141/1645-12, doi:10.3141/1645-12.
Prashker, J.N., Bekhor, S., 2000. Congestion, stochastic, and similarity effects in stochastic user equilibrium. Transportation Research Record 1733, 80–87. URL: https://dx.doi.org/10.3141/1733-11, doi:10.3141/1733-11.
Prato, C.G., Bekhor, S., 2006. Applying branch and bound techniques to route choice set generation. Transportation Research Record , 19–28URL: https://dx.doi.org/10.3141/1985-03, doi:10.3141/1985-03.
Saeedmanesh, M., Geroliminis, N., 2016. Clustering of heterogeneous networks with directional flows based on "snake" similarities. Transportation Research Part B: Methodological 91, 250–269. URL: https://dx.doi.org/10.1016/j.trb.2016.05.008, doi:10.1016/j.trb.2016.05.008.
Saeedmanesh, M., Geroliminis, N., 2017. Dynamic clustering and propagation of congestion in heterogeneously congested urban traffic networks. Transportation Research Procedia 23, 962–979. URL: https://dx.doi.org/10.1016/j.trb.2017.08.021, doi:10.1016/j.trb.2017.08.021.
Sbayti, H., Lu, C.C., Mahmassani, H.S., 2007. Efficient implementation of method of successive averages in simulation-based dynamic traffic assignment models for large-scale network applications. Transportation Research Record: Journal of the Transportation Research Board 2029, 22–30. URL: https://dx.doi.org/10.3141/2029-03, doi:10.3141/2029-03.
Shafiei, S., Gu, Z., Saberi, M., 2018. Calibration and validation of a simulation-based dynamic traffic assignment model for a large-scale congested network. Simulation Modelling Practice and Theory 86, 169–186. URL: https://dx.doi.org/10.1016/j.simpat.2018.04.006, doi:10.1016/j.simpat.2018.04.006.
Shao, H., Lam, W., Meng, Q., Tam, M., 2006. Demand-driven traffic assignment problem based on travel time reliability. Transportation Research Record 1985, 220–230. URL: https://dx.doi.org/10.3141/1985-24, doi:10.3141/1985-24.
Shao, H., Lam, W.H.K., Tam, M.L., 2006. A reliability-based stochastic traffic assignment model for network with multiple user classes under uncertainty in demand. Networks and Spatial Economics 6, 173–204. URL: https://dx.doi.org/10.1007/s11067-006-9279-6, doi:10.1007/s11067-006-9279-6.
Sheffi, Y., 1985. Urban Transportation networks: Equilibrium Analysis with Mathematical Programming Methods. Prentice Hall Inc., United States of America. chapter 10 and 11.
Simon, H.A., 1957. A behavioral model of rational choice. Wiley, New York.
Simon, H.A., 1966. Theories of Decision-Making in Economics and Behavioural Science. Palgrave Macmillan UK, London. pp. 1–28. URL: https://dx.doi.org/10.1007/978-1-349-00210-8_1, doi:10.1007/978-1-349-00210-8_1.
Simon, H.A., 1990. A mechanism for social selection and successful altruism. Science 250, 1665–1668. URL: https://dx.doi.org/10.1126/science.2270480, doi:10.1126/science.2270480.
Simon, H.A., 1991. Bounded rationality and organizational learning. Organization Science 2, 125–134. URL: https://dx.doi.org/10.1287/orsc.2.1.125, doi:10.1287/orsc.2.1.125.
Small, K.A., 1982. The scheduling of consumer activities: Work trips. The American Economic Review 72, 467–479. URL: http://www.jstor.org/stable/1831545.
Smith, M., 1979. The existence, uniqueness and stability of traffic equilibria. Transportation Research Part B: Methodological 13, 295 – 304. URL: https://dx.doi.org/10.1016/0191-2615(79)90022-5, doi:10.1016/0191-2615(79)90022-5.
Szeto, W.Y., Lo, H.K., 2006. Dynamic traffic assignment: properties and extensions. Transportmetrica 2, 31–52. URL: https://dx.doi.org/10.1080/18128600608685654, doi:10.1080/18128600608685654.
Taale, H., 2008. Integrated Anticipatory Control of Road Networks A Game Theoretical Approach. Ph.D. thesis. Phd thesis Delft University of Technology. Delft, The Netherlands.
van der Zijpp, N.J., Catalano, S.F., 2005. Path enumeration by finding the constrained k-shortest paths. Transportation Research Part B: Methodological 39, 545–563. URL: https://dx.doi.org/10.1016/j.trb.2004.07.004, doi:10.1016/j.trb.2004.07.004.
Vickrey, W., 2020. Congestion in midtown manhattan in relation to marginal cost pricing. Economics of Transportation 21, 100–152. URL: https://dx.doi.org/10.1016/j.ecotra.2019.100152.
Viti, F., Tampère, C.M.J., 2010. New Developments in Transport Planning: Advances in Dynamic Traffic Assignment. Edward Elgar, Cheltenham UK. chapter Dynamic Traffic Assignment: Recent Advances and New Theories Towards Real Time Applications and Realistic Travel Behaviour. URL: https://doi.org/10.4337/9781781000809.00007, doi:10.4337/9781781000809.00007.
Wang, J.Y.T., Ehrgott, M., Chen, A., 2004. A bi-objective user equilibrium model of travel time reliability in a road network. Transportation

Research Part B: Methodological 66, 4–15. URL: https://dx.doi.org/10.1016/j.trb.2013.10.007, doi:10.1016/j.trb.2013.10.007.

Wardrop, J.G., 1952. Some theoretical aspects of road traffic research. Institution of Civil Engineering 1, 325–362. URL: https://dx.doi.org/10.1680/ipeds.1952.11259, doi:10.1680/ipeds.1952.11259.

Watling, D., 2006. User equilibrium traffic network assignment with stochastic travel times and late arrival penalty. European Journal of Operational Research 175, 1539–1556. URL: https://dx.doi.org/10.1016/j.ejor.2005.02.039, doi:10.1016/j.ejor.2005.02.039.

Wie, B.W., Tobin, R.L., Carey, M., 2002. The existence, uniqueness and computation of an arc-based dynamic network user equilibrium formulation. Transportation Research Part B 36, 897–918. URL: https://dx.doi.org/10.1016/S0191-2615(01)00041-8, doi:10.1016/S0191-2615(01)00041-8.

Yildirimoglu, M., Geroliminis, N., 2014. Approximating dynamic equilibrium conditions with macroscopic fundamental diagrams. Transportation Research Part B: Methodological 70, 186–200. URL: https://dx.doi.org/10.1016/j.trb.2014.09.002, doi:10.1016/j.trb.2014.09.002.

Zhang, K., Mahmassani, H.S., Lu, C.C., 2013. Dynamic pricing, heterogeneous users and perception error: Probit-based bi-criterion dynamic stochastic user equilibrium assignment. Transportation Research Part C: Emerging Technologies 27, 189 – 204. URL: https://dx.doi.org/10.1016/j.trc.2012.05.001, doi:10.1016/j.trc.2012.05.001. selected papers from the Seventh Triennial Symposium on Transportation Analysis (TRISTAN VII).

Zhu, S., Levinson, D., 2015. Do people use the shortest path? an empirical test of wardrop's first principle. PLoS ONE , 1–18URL: https://dx.doi.org/10.1371/journal.pone.0134322, doi:10.1371/journal.pone.0134322.